RADIATION TRANSPORT SIMULATION STUDIES USING MCNP FOR A COW PHANTOM TO DETERMINE AN OPTIMAL DETECTOR CONFIGURATION FOR A NEW LIVESTOCK PORTAL

A Thesis

by

JOE JUSTINA

Submitted to the Office of Graduate Studies of
Texas A&M University
in partial fulfillment of the requirements for the degree of

MASTER OF SCIENCE

August 2012

Major Subject: Nuclear Engineering

RADIATION TRANSPORT SIMULATION STUDIES USING MCNP FOR A COW PHANTOM TO DETERMINE AN OPTIMAL DETECTOR CONFIGURATION FOR A NEW LIVESTOCK PORTAL

A Thesis

by

JOE JUSTINA

Submitted to the Office of Graduate Studies of
Texas A&M University
in partial fulfillment of the requirements for the degree of

MASTER OF SCIENCE

Approved by:

Co-Chairs of Committee,	Craig M. Marianno
	Sunil S. Chirayath
Committee Members,	William S. Charlton
	Sunil P. Khatri
Head of Department,	Yassin A. Hassan

August 2012

Major Subject: Nuclear Engineering

ABSTRACT

Radiation Transport Simulation Studies Using MCNP for a Cow Phantom to Determine an Optimal Detector Configuration for a New Livestock Portal.

(August 2012)

Joe Justina, B.S., University of Mysore; M.Sc., Mangalore University

Co-Chairs of Advisory Committee: Dr. Craig M. Marianno
Dr. Sunil S. Chirayath

A large radiological accident will result in the contamination of surrounding people, animal, vegetation etc. In such a situation assessing of the level of contamination becomes necessary to plan for the decontamination. There are plans existing for evaluating contamination on people. However, there are limited to no plans to evaluate animals. It is the responsibility of the United States Department of Agriculture (USDA) to decontaminate animals. So the objective of this thesis work was to design a scalable gamma radiation portal monitor (RPM) which can be used to assess the level of contamination on large animals like cattle. This work employed a Monte Carlo N-Particle (MCNP) radiation transport code for the purpose. A virtual system of cow, radiation source representing the contamination, cattle chute and different detector configurations were modeled. NaI scintillation detectors were modeled for this work. To find the optimal detector size and configuration, different detector orientations were simulated for different source positions using the MCNP code. Also simulations were

carried out using different number and size of the detectors. It was found that using 2” x 4” x 16” detector yielded a minimum detectable activity (MDA) value of 0.4 μCi for ^{137}Cs source.

ACKNOWLEDGEMENTS

I would like to thank my advisors Dr. Craig M. Marianno and Dr. Sunil S Chirayath for all their help and guidance throughout this work. Dr. Sunil Chirayath has helped me with all the MCNP related work. Also I thank Dr. William S. Charlton for his valuable suggestions in completing this thesis work. I would also like to thank my committee member Dr. Sunil P. Khatri for his suggestions.

I also would like to thank Dr. Alexander Solodov for lending me the background source term and Dr. Andy Herring for providing me the information needed to model the cow.

I am also thankful to the following people for their moral support: Mr. Nandan Chandregowda, Dr. Sunil S. Chirayath, Dr. Paul Nelson, and my dear family members. It wouldn't have been possible for me to complete my thesis without their support and encouragement.

TABLE OF CONTENTS

CHAPTER Page

LIST OF FIGURES

FIGURE Page

LIST OF TABLES

CHAPTER I

INTRODUCTION

I.A. Background

A radiological incident such as a nuclear power plant disaster, detonation of a nuclear explosive device or radiological dispersal device will result in the release of a plume of radioactive particles into the atmosphere. The blast will carry the particles into the surrounding area contaminating people, animals, vegetation, etc. In an accident like this, it is necessary to evaluate the level of radioactive contamination for effectively carrying out the decontamination procedures. There are plans and procedures to evaluate and assess the level of contamination in the case of human beings. However, there are only minimal such plans in the case of animals.

Why should animals be considered during such an accident? This question can be answered by classifying animals into pets and livestock for the purpose of this thesis. Many people have close affection for their pets and they don't want to abandon them during evacuation in the event of an accident. They can risk their own lives to protect their pet from any harm[1]. Conversely, livestock contribute to a large part of the country's economy. Table I illustrates the importance of the beef industries to the U.S. economy[2]. In Texas State alone, cattle make up an $8 billion industry; therefore it is essential to develop an effective method to evaluate the extent of radioactive contamination on

---

This thesis follows the style of *Nuclear Technology*.

livestock after a radiological accident[3]. The effect on the diary and meat industries will be devastating if reliability of the product comes into question due to contamination concerns.

TABLE I

Statistical information on the U.S. beef and cattle industry for the year 2010[4].

Retail equivalent value of U.S. beef industry	$74 billion
Total U.S. beef consumption	26.4 billion pounds
Value of U.S. cattle and calf production	$37.0 billion
U.S. beef production (commercial carcass weight)	26.41 billion pounds
U.S. beef exports (commercial carcass weight and value)	2.3 billion pounds, $3.839 billion
U.S. beef exports as percent of production	8.7 percent

The National Response Framework (NRF) states the roles and responsibilities of the local, tribal, State and Federal governments in any accident situation, including a radiological accident. One of the responsibilities is to ensure that the local emergency plans take into account, the decontamination, evacuation and rescue of animals too[5]. It is the responsibility of the United States Department of Agriculture (USDA) to evaluate the level of radioactive contamination, decontaminate the animals, and provide support for stabilization and disposition of contaminated animal carcasses[5, 6]. In response, the USDA has funded this project to develop a portable, scalable gamma radiation portal monitor (RPM) which can be used for livestock. This thesis involves the development of

a design concept for a mission flexible portal monitor that can be employed to scan livestock.

The radioactive materials license issued to the USDA by the National Regulatory Commission (NRC) requires knowing the minimum detectable activities (MDA) of the instruments used for detecting radiation[7]. The MDA is an indicator of how well the instrument can measure small amounts of radioactivity typically detected during radiation contamination monitoring.

Previously, an animal portal monitor was designed which could be used to scan household pets for radioactive contamination[8]. It was a scalable system of up to 4 scintillation detectors and used custom software to determine the level and relative position of contamination. But, the size of that portal was small and cannot be used for assessing the radioactive contamination of large animals. As an alternative to this small system, this project work focuses on a way to determine contamination on large animals such as cattle.

I.B. Objectives

This work is the first phase of a project to develop a radiation portal monitor (RPM) for livestock. This RPM would be employed following a large scale accident resulting in a release of radioactive material. The objective of this project is to employ a computer simulation to evaluate the optimal detector configuration required to detect point or surface contamination on livestock due to gamma emitting radioisotopes. This includes the determination of the optimal size, its placement and detector material

composition. Monte Carlo N-Particle (MCNP) radiation transport code[9] was used for the simulation. Using the results of this work a theoretical minimum detectable activity (MDA) will be determined for different radiation detector configurations of the RPM.

I.C. Choice of Detectors

Several factors should be considered when selecting the detectors for RPMs and the choice depends on the application of the portal. A RPM employed to scan livestock should effectively assess the contamination level, location of the contamination, and identify the radionuclides present in order to plan for decontamination. Level and location of contamination are important to decide on the decontamination procedures to be followed. There are two clean up procedures followed- partial and complete veterinary cleanup. Partial decontamination consists of cleaning up external openings of alimentary and respiratory channels and their immediate vicinity in order to prevent animal from ingesting the radioactive material. Complete veterinary cleanup includes decontamination of entire body surface of the animal. The chief criterion to decide if a complete veterinary cleanup is needed is by assessing the level of contamination. The waste that is generated out of the cleaning has to be handled appropriately as radioactive wastes.

Isotope identification is important because this may influence decontamination procedures or may determine the viability of the animal to return to the food chain. The selection of the method of decontamination is based on the nature of the contaminant nuclide. The most frequently used decontamination procedure is to wash the

contaminated surface with soap and water. But, soap itself may not be the best agent because it is alkaline in nature that tends to transform radionuclides into colloidal form. Material in colloidal form gets adsorbed into the skin making it difficult to remove[10]. There are ion specific radioactive decontamination solutions (RDS) available for use[11], for example, pentacine and dimethylsulfoxide is effective in removing ^{241}Am.

The common detector materials used for gamma detection purpose include sodium iodide (NaI) detectors, polyvinyltoluene (PVT), and High Purity germanium (HPGe) detectors. However, PVT and NaI are the ones preferred for portal monitors. The factors that influence the choice of the detectors for the RPM include:

- Ease to fabricate large area detectors
- Ability to withstand physical changes and environmental stress
- Cost
- High intrinsic efficiency

PVT is a plastic scintillator and is produced by dissolving an organic monomer (vinyl toluene) in a solvent and then subsequently polymerized to get a solid plastic[12]. The ease with which it can be manufactured has made the plastic scintillator an extremely useful scintillator material. It can be formed into different shapes and sizes making it popular in places where large detectors are required. Usually RPMs employ plastic scintillators because a large area provides more uniform detection sensitivity[13]. Other advantage of using PVT is the small pulse decay time of 2.4 ns[12]. The approximate cost of (3.8 cm x 36 cm x 173 cm) plastic detector is about $2000 as compared to about $6000 for a (5 cm x 10 cm x 41cm) NaI detector[14]. However it has low detection

efficiency as compared to NaI or any other inorganic detectors. The effective atomic number of plastic scintillator is very low (Z_{eff}≈4.5) because of its low atomic number constituents. As a result, there is low photoelectric effect (gamma ray interaction mechanism of interest) cross section for gamma ray of typical energies. Thus a spectrum obtained from a plastic scintillator is dominated by Compton interactions which provide little information on energy of the detected photons, thereby making radionuclide identification difficult. There have been attempts made to increase the Z_{eff} by doping the organic plastic with heavy metals[15] but the poor solubility of the high Z element and quenching luminescence were never resolved[16].

NaI is an inorganic scintillator material and the most widely used detector for routine gamma ray spectroscopy. It has a higher light yield (photons/keV) and effective atomic number of NaI is higher, (Zeff≈49.7) compared to PVT. The gamma energy spectrum obtained by this detector show photo-peaks which can be used to identify the isotopes responsible for contamination. Like PVT, the crystal can be grown and pressed to form any size and shape so that large size detectors can be fabricated[12]. It is also inexpensive as compared to HPGe detectors. However, NaI has poor resolution as compared to HPGe detectors because the energy required to produce a photoelectron at the photocathode of the photomultiplier tube is about 170eV[17]. This number is much lower for an HPGe detector which is discussed in the following paragraph. Apart from this, the problem with this detector is that the NaI crystal is hygroscopic and fragile. It is sensitive to temperature variation and easily prone to damage. The decay time is large (230 ns) as compared to PVT.

HPGe detector is a semiconductor detector manufactured by reducing the impurity level in the germanium (Ge) to a level less than 10^9 atoms/cc[12]. This high purified Ge crystal has high resistance and a depletion layer of up to 10 mm thick can be achieved if reverse bias voltage is applied. This depletion layer acts as a solid ionization chamber. The energy required to produce an ion pair is only 2.96 eV[18]. Any radiation of energy greater than 2.96 eV entering the depletion region produces electron-hole pairs which in turn induces a current flow. Hence, the detector has high resolution as compared to NaI. The Z_{eff} of Ge is lower than NaI and hence the photoelectric absorption cross section is lower. Hence, the efficiency of HPGe is lower than NaI. But, it is greatly compensated by the resolution of the detector. However, there is a major disadvantage using this detector in a portal monitor. The detector must be operated at liquid nitrogen temperatures in order to avoid any noise arising due to lowered resistance in room temperature. This requirement of liquid nitrogen makes this detector less preferred for field use. Also, the energy required to create an electron-hole pair is dependent on the temperature and hence maintaining temperature is very important. Another disadvantage is that developing a large HPGe crystal is expensive.

The above comparison suggests that NaI detector is preferred. This material is relatively inexpensive, can be fabricated into large sizes and can be used for isotope identification. As a result, NaI detectors were used for the radiation transport simulations reported in this thesis.

I.D. Use of MCNP Transport Code

A computer simulation allows studying the behavior of a system in a virtual world. This provides a relatively cheap, time efficient means to check and optimize the system for its performance before it can be taken into the real world. This thesis work is mainly done using MCNP radiation transport code. The Monte Carlo simulation is one of the numerical methods of computer simulations. It can be used to simulate and solve problems of neutron, photon, electron, or coupled neutron/ photon/ electron transport through material medium.. The main advantage of MCNP is that it can be used to model complex problems (such as the one handled here in the thesis work), which is not amenable by deterministic transport methods.

MCNP is a versatile radiation transport code. Its main features include the data of nuclear reaction cross section libraries, various source specifications, tallies (detector responses), estimation of precision of the predictions, variance reduction techniques, etc.. Nuclear data table exists for neutron interactions, photon interactions, neutron induced photons, neutron dosimetry or activation, and thermal particle scattering S (α, β). Photon interaction table exists for elements with atomic number ranging from $Z=1$ to $Z=100$. User can specify the data table to be used. MCNP allows the user to define the source geometry, position, direction, energy, and time. It also allows assigning probabilities on each of them without changing the code. In addition to this, source biasing can be done by special built-in functions to improve statistics of tallies.

Yet another feature of MCNP includes specifying tallies. The user can instruct MCNP to give specific tallies like particle current, particle flux, and energy deposition.

All tallies are normalized to be per starting particle. These tallies are functions of the time and energy specified by the user. Along with the tally table, MCNP code output will have a summary table which helps in understanding the physics of the problem. If encountered with an error while running the code then a detailed diagnostics will be printed which will be helpful for debugging.

Along with the tallies, the MCNP output will have the relative standard error printed next to the results. These are 1-σ deviation of the mean divided by the estimated mean. These errors can be used to make confidence intervals around the estimated mean. In addition to the relative standard error, MCNP also calculates the figure of merit (FOM). FOM gives the user an idea about the correctness of the confidence interval.

As mentioned earlier, MCNP allows user to specify a tally. In this work F8, a pulse height tally was used. It provides the energy distribution of the pulses that are created within the cell that models the detector. The tally value corresponds to the counts registered in each energy bin specified by the user. The tally results are normalized to be per starting particle. Hence, multiplication of the tally value with the source strength (particles per second) and its branching ratio results in the count rate registered in the detector.

$$f(E)=Ce^{-\left(\frac{E-E_0}{A}\right)^2} \quad (1)$$

where E = the broadened energy,

E_0 = the unbroadened energy of the tally,

C = a normalization constant,

A = the Gaussian width.

The Gaussian width is related to the full width at half maximum (FWHM) (Eq. 2). The desired FWHM is specified by the user using parameters a, b, c which are related to FWHM as in Eq. 3. These parameters are functions of the type of detector and the size of the detector.

$$A = \frac{FWHM}{2\sqrt{\ln 2}} \quad (2)$$

$$FWHM = a + b\sqrt{E + cE^2} \quad (3)$$

I.E. Choice of Source Representing Contamination

Radionuclides can be released to the environment during nuclear accidents/incidents. Table II summarizes the radionuclides of concern released from different activities. ^{137}Cs is nuclide that may be released in almost every kind of accident. ^{137}Cs is long lived nuclide with a half-life of 30 years. It decays via emission of β particles to ^{137}Ba which then goes to ground state by emitting a 0.662 MeV gamma radiation. Contamination due to β emitters cause skin burns. Also, ^{137}Cs, when ingested are absorbed into the circulatory system and can be fatal if not treated. Because of the importance of this radio-isotope, radiation transport simulations reported here employed 5 μCi ^{137}Cs source.

TABLE II

Radionuclides released during accidental situations that are of most concern[19,20].

Accident	**Radionuclides of most concern**
Nuclear reactor	^{131}I, ^{134}Cs, ^{137}Cs, ^{103}Ru, ^{106}Ru, ^{90}Sr
Nuclear fuel reprocessing plant	^{90}Sr, ^{137}Cs, ^{239}Pu, ^{241}Am
Nuclear waste storage facilities	^{90}Sr, ^{137}Cs, ^{239}Pu, ^{241}Am
Nuclear weapons	^{239}Pu
RDD[16]	^{241}Am, ^{60}Co, ^{137}Cs, ^{252}Cf, ^{90}Sr, ^{226}Ra, ^{192}Ir, ^{210}Po

CHAPTER II

METHODOLOGY

II.A. Procedure

The steps involved in simulating the complex geometry of this problem in MCNP include:

1. Developing the model of a cow phantom using MCNP

2. Developing MCNP model of cattle chute and detectors

3. Performing MCNP radiation transport simulations to find optimal detector configuration and

4. Determining the minimum detectable activity (MDA) for each configuration.

II.B. Developing a Cow Phantom Model using MCNP

The physical attributes of the cow were collected from the collaborators of Animal Science Department and is presented in TABLE III (Dr. Andy Herring, personal communication, February 2011). All these measurements are of a typical mature cow weighing 1200 lbs. Other physical attributes including bone and muscle density were collected through literature[21]. Each part of the cow was represented by different geometrical shapes. In the model, abdominal region was represented by an ellipsoid, neck was modeled as an oblique cone, head was represented by a cone and legs were

simulated as cylinders and cones. Each surface is defined by an equation[22, 23]. The following section describes the equations that were used to represent each surface.

TABLE III

Physical dimensions of a mature cow weighing 1200 lbs.

Body Part	**Dimension (cm)**
Hip height	132.1
Body depth	66.0
Lower leg circumference	30.5
Neck depth in middle	43.2
Neck circumference	121.9
Body length (nose to tail)	144.8

II.B.1. Abdomen Represented by an Ellipsoid

The shape of an ellipsoid was picked to represent the cow's abdomen. To define this shape in MCNP, Eq. 4 was employed. In MCNP, any geometry is defined using a set of cell definitions and surface definitions. For an ellipsoid, the cell definition and surface definition were written as,

```
Cell definition: 1 -0.915 -1 -2 3
```

which means the cell is filled with material 1 (defined in data section of the MCNP input) whose density is 0.915 gcm^{-3} and contained in the region intersected by surfaces 1, 2 and 3.

```
Surface definition:

1 sq A B C D E F G x y z


2 px 54

3 px -54
```

A surface defining an ellipsoid consists of the parameters A, B, C, D, E, F and G found in Eq. 4. These unknown parameters were found by solving a set of simultaneous equations. The value of A was assumed to be equal to 1 for simplicity and then remaining 6 unknowns were determined. The simultaneous equations were written by using 6 different values of x, y, z which are marked on Fig. 1. These values were chosen such that they lie on the surface of the desired ellipsoid. The physical dimensions in TABLE III were used to choose these x, y, z values. Four of these points were selected such that the points lie on the circumference of the cross section of the ellipsoid at the center. The other two points were obtained by knowing the points that should lie on the circumference of the circular cross sections at the ends of the ellipsoid where it is intersected by the planes. In this model the body depth or the diameter of the circular cross section of the ellipsoid was 66 cm at the center and 51.2 cm at the ends (Fig. 2).

$$A(x-\bar{x})^2+B(y-\bar{y})^2+C(z-\bar{z})^2+2D(x-\bar{x})+2E(y-\bar{y})+2F(z-\bar{z})+G=0 \qquad (4)$$

Where A, B, C, D, E, F and G are the input parameters,

x, y, and z are the points lying on the ellipsoid.

$\bar{x}$,$\bar{y}$,and $\bar{z}$ are the X, Y, and Z coordinates of the center of the ellipsoid.

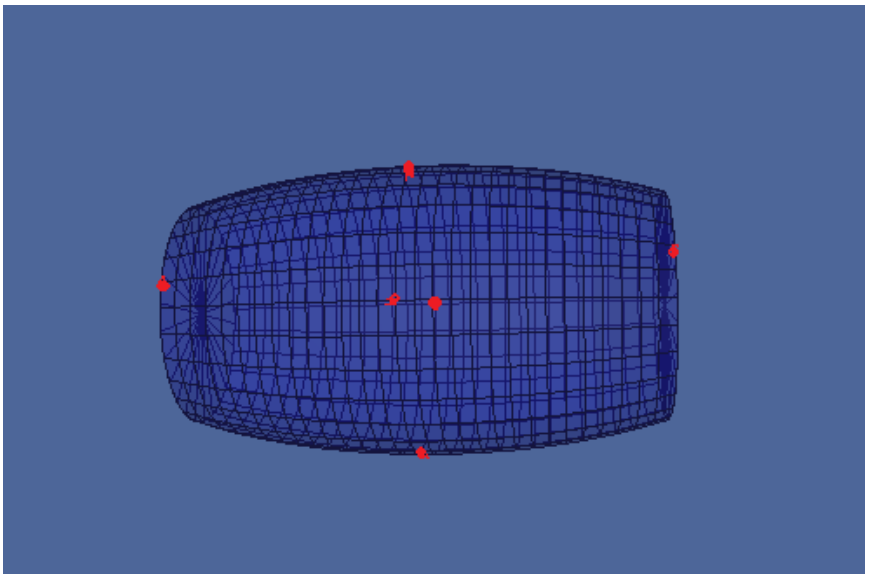

Fig. 1: 3D model of the ellipsoid generated by MCNP VISED Software. The points marked in red were the points considered to find the equation.

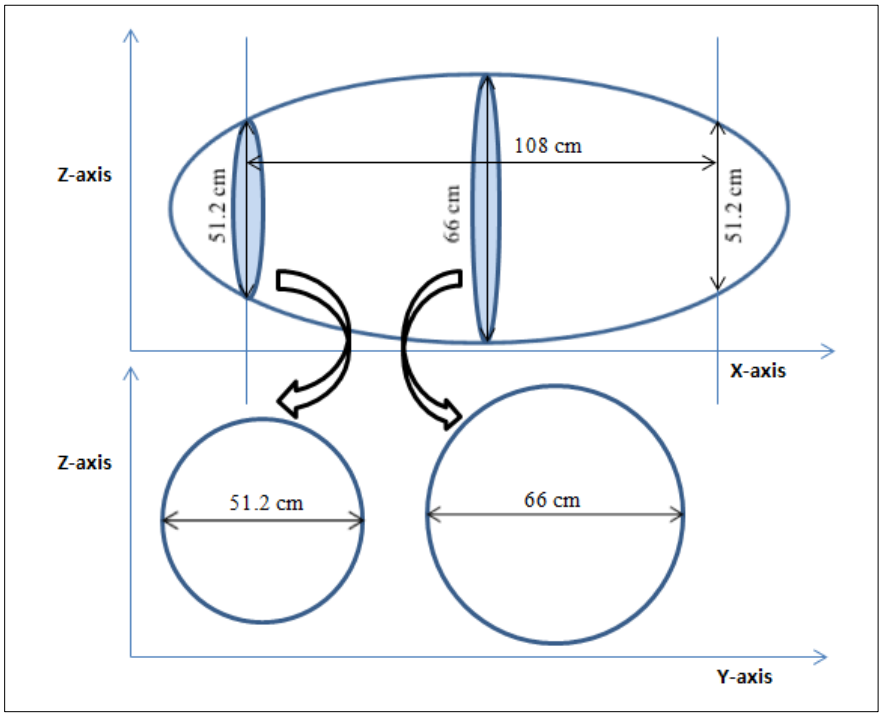

Fig. 2: Section of the ellipsoid showing the dimensions used in the cow model.

II.B.2. Neck Represented by an Oblique Frustum

The neck was represented by a general cone. The cell definition and surface definition were written as,

```
Cell definition: 1 -0.915 4 2 -5
```

Indicating the neck is filled with material 1 of 0.915 g/cc density and is bound by the surfaces defined by 2, 4 and 5.

```
Surface definition:

4     gq A B C D E F G H J K

2     px 54

5     px 73
```

A surface defining an oblique cone consists of the parameters A, B, C, D, E, F, G, H, J and K found in Eq. 5. These parameters were found in a similar way that was used to find the parameters of ellipsoid. Here 9 equations were used to find the 9 unknown parameters. The resulting cone was then cut by a plane to form a frustum whose height was 19 cm and the diameter of the base was 51.2 cm as shown in Fig. 3. The 3D image of the cone was not generated by MCNP Visual editor Software (VISED).

$$Ax^2+By^2+Cz^2+Dxy+Eyz+Fzx+Gx+Hy+Jz+K=0 \quad (5)$$

Where A, B, C, D, E, F, G, H, J, and K are unknown parameters,

x, y, and z are the points that lie on the cone.

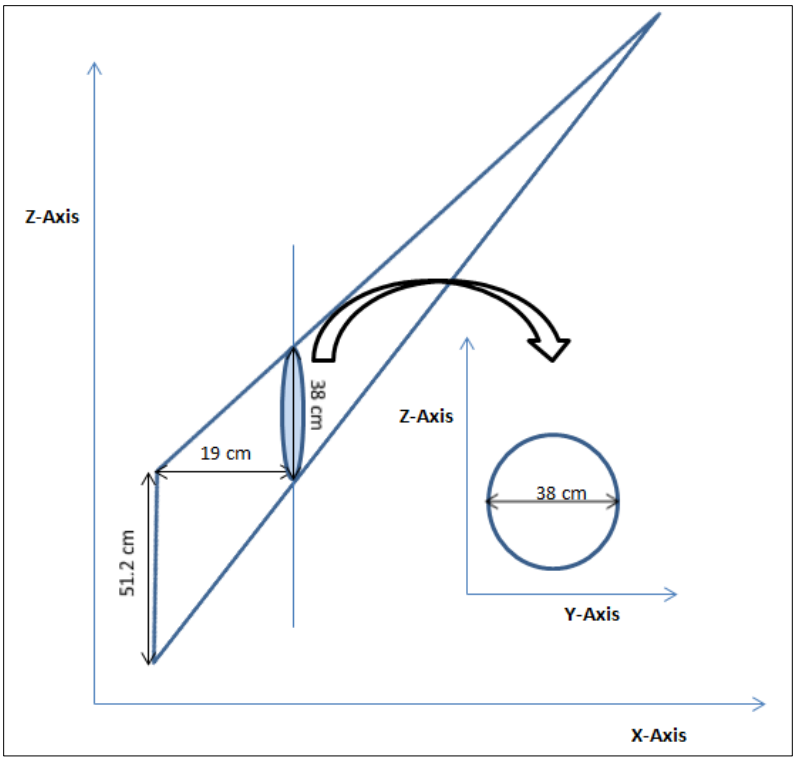

Fig. 3: Section of the cone representing the neck showing the dimensions.

II.B.3. Head Represented by a Right Circular Frustum

The head was represented as a right circular frustum. In MCNP a cone whose axis is parallel to the X-axis is defined using the surface mnemonic k/x followed by the parameters x, y, z of the vertex and the square of the tangent of the opening angle of the cone, t^2. Again, each parameter was found according to the dimension of the head of the cow. The cone was then cut by a plane to form a frustum as shown in Fig. 3. The frustum was thus return using the surface dimensions,

(1) k/x x y z t^2±1 and (2) px x

The k/x mnemonic will generate two sheet cone which means there will two cones opening from the vertex in opposite directions. ±1 is used to specify any one of the cones. Since in the input a plane is used to cut the cone ±1 may not be included.

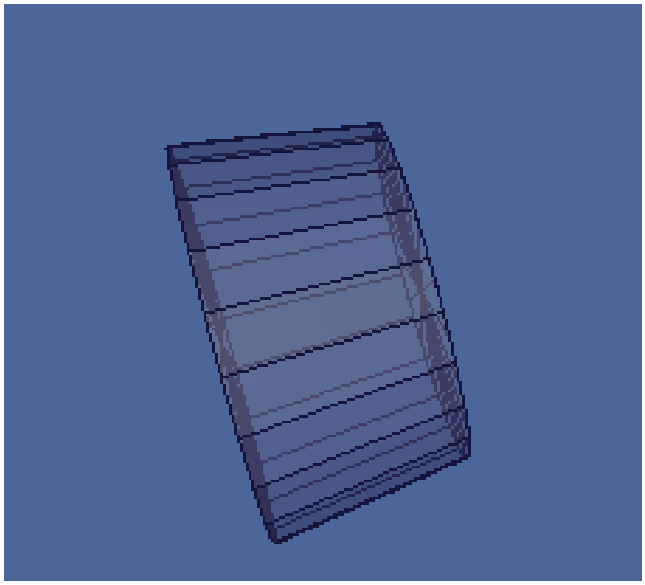

Fig. 4: 3D image of the frustum generated by MCNP VISED

II.B.4. Legs Represented by Cylinders and Frustums

The lower part of the leg was represented by a right circular cylinder and the upper part by a frustum as seen in Fig. 5. The cylinder was defined using the surface mnemonic c/z which means that the cylinder has its axis parallel to the Z axis. The radius and the center of the cylinder included in this definition were consistent with the physical attributes of the animal. The three surface definitions used for representing the legs were,

(1) c/z x y R (cylinder parallel to Z axis) representing lower part of the leg

(2) k/z x y z t^2±1 (cone with axis parallel to Z axis) representing upper part of the leg.

(3) pz z (plane cutting Z axis at z)

Here, in the case of a cylinder, x, y were the X and Y coordinates of its center and R was the radius. For the cone, x, y, z were the coordinates of the cone's vertex and t^2 was the square of the tangent of the opening angle of the cone. ±1 was used to specify one sheet cone.

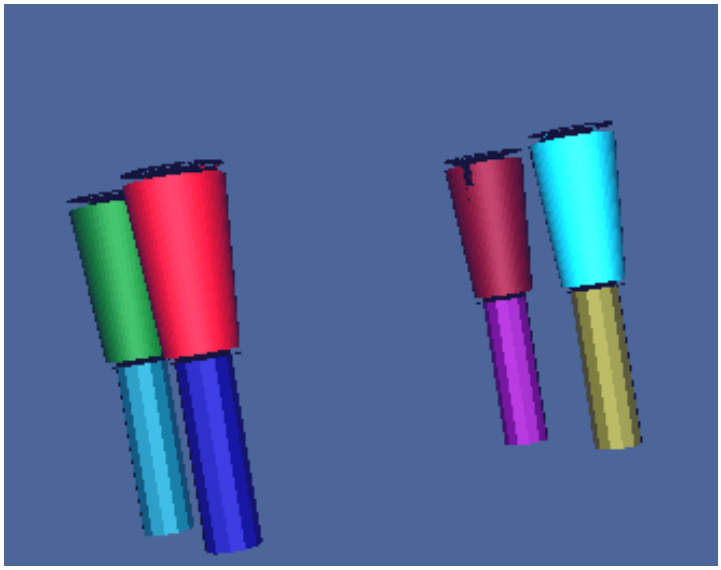

Fig. 5: 3D image of the legs generated by MCNP VISED.

II.B.5. Internal Structures of the Cow Model

The internal structures included the vertebral column, ribcage and the shoulder blades. The vertebral column was a cylinder parallel to the X axis. The neck vertebra was modeled as a cylinder but was rotated by an angle 60 degrees about Y axis. The

ribcage was modeled by defining a set of concentric cylinders. These cylinders were intersected by planes at varying distances in order to form ring like structures as shown in Fig. 6. The shoulder blades were modeled as a polyhedron by defining a set of planes that bound the polyhedron.

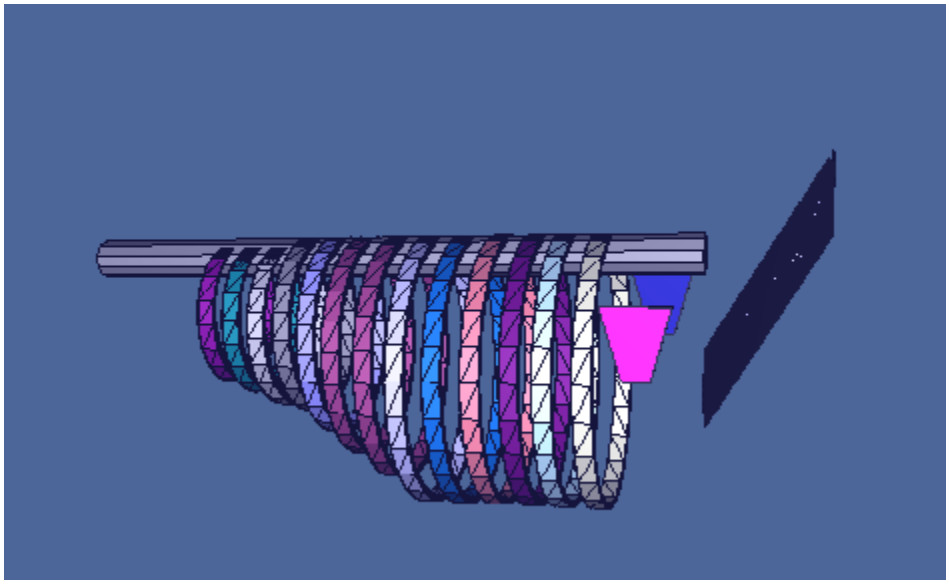

Fig. 6: 3D view of the vertebral column, ribcage, shoulder blade and neck vertebra.

II.C. Modeling of the Chute

Handling animals during decontamination procedure is much more difficult than human beings. The traumatized animals tend to escape, cause injury to the persons handling them or even break the detector set up. Hence, it is necessary that animals be guided through a chute. Therefore, a cattle chute was modeled, which can be used to guide the animal move through without causing damage to any people, objects surrounding or itself. It was assumed that the cow would be contained within a chute

during scanning which allowed the animal to be somewhat localized. The chute modeled was a SILENCER hydraulic squeeze chute shown in Fig. 7. The dimensions of the chute were measured using measuring tape. These measured dimensions were used to model the chute in MCNP. The whole chute was modeled using cylinders and planes. Fig. 8 shows the MCNP model of the chute. The material of the chute was steel, exact composition was unknown. However, steel is mostly composed of iron and hence in the model iron was used.

Fig. 7: Commercially available SILENCER hydraulic squeeze chute.

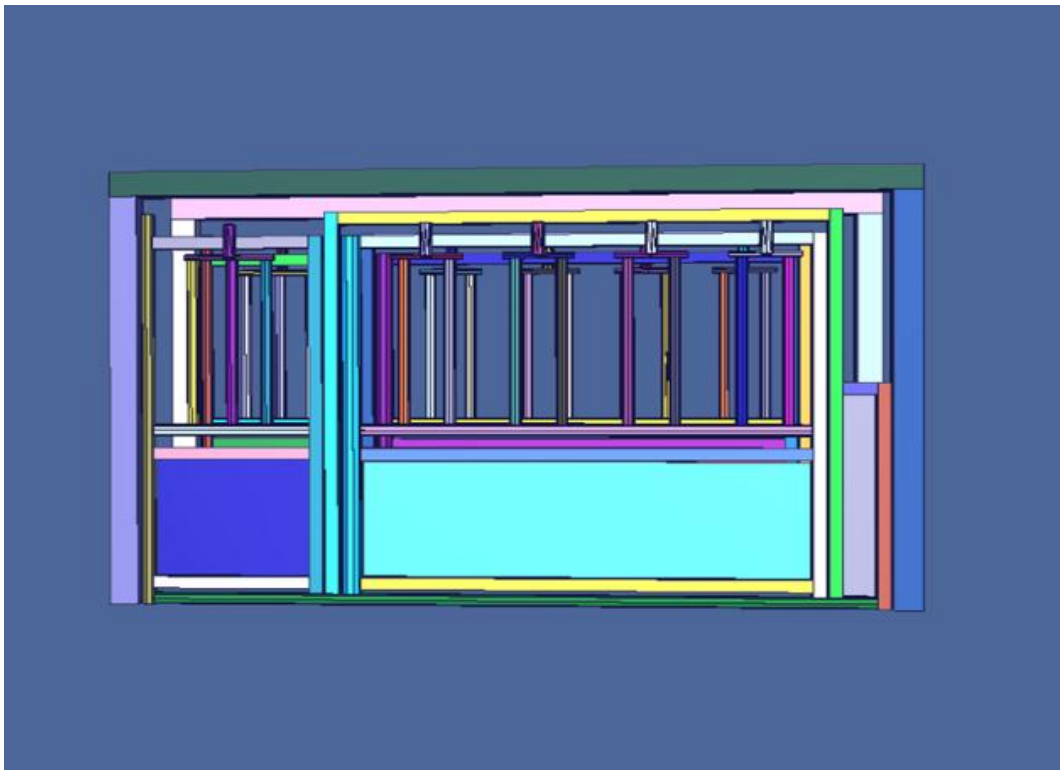

Fig. 8: 3D model of the cattle chute generated by MCNP VISED.

II.D. Modeling of the Detectors

The NaI detectors were modeled as cuboids. In MCNP, cuboids are defined by a set of planes that bound the cuboid. Two different sized detectors were modeled. One was a 2” ×4” ×4” detector and the other was 2” ×4” ×16” detector. The detectors were placed six inches away from the cow.

II.E. Material Definition in the Model

Compositions of materials used in the simulations were retrieved from literature. The cow model was composed of soft tissue material and bone material. For soft tissue,

the material definition included hydrogen, oxygen and small percent of carbon and nitrogen. For bone, the material definition consisted of the atom fraction values of the elements that constitute the bone material. The inorganic composition is formed by carbonated hydroxyapatite ($Ca_{10}(PO_4)_6(OH)_2$). The chute material was composed of iron. The detectors were modeled as composing of sodium and iodine in 1:1 atom ratio.

II.F. MCNP Runs with Single and Multiple Sources

Initial simulations, included only a cow and the detectors. The first simulation used a 5 μCi ^{137}Cs point source which emits 662 keV gamma radiation with a branching ratio of 0.85, positioned at the center of the abdominal region and the detector was placed about six inches away from the cow. The source position was varied to five different positions – four near abdominal region and one on the nose. These five positions were chosen such that it represented a contamination anywhere on the body of the cow. The detector dimensions used in this case was 2" ×4" ×16", where the 2" ×16" side was parallel to the ground as shown in Fig. 9. The detectors were placed on one side of the cow assuming that the response would be symmetric for detectors placed on the other side of the cow. Next set was performed by changing the detector orientation such that the 2" ×16" face was perpendicular to the ground as shown in Fig. 10. A comparison of the parallel and perpendicular orientation of the detectors was done.

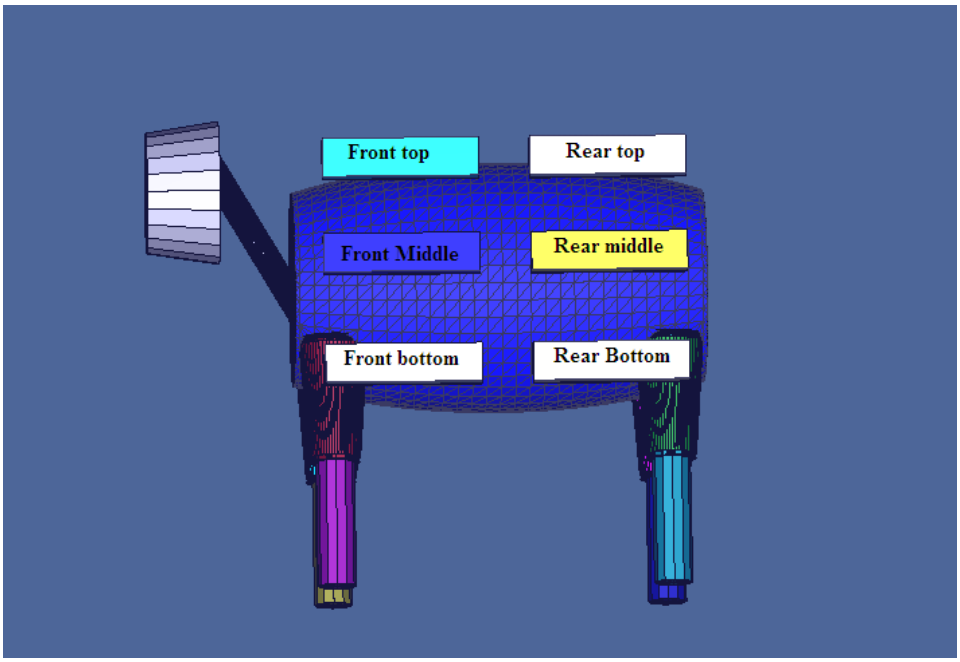

Fig. 9: Detectors placed parallel to the ground with the positions labeled.

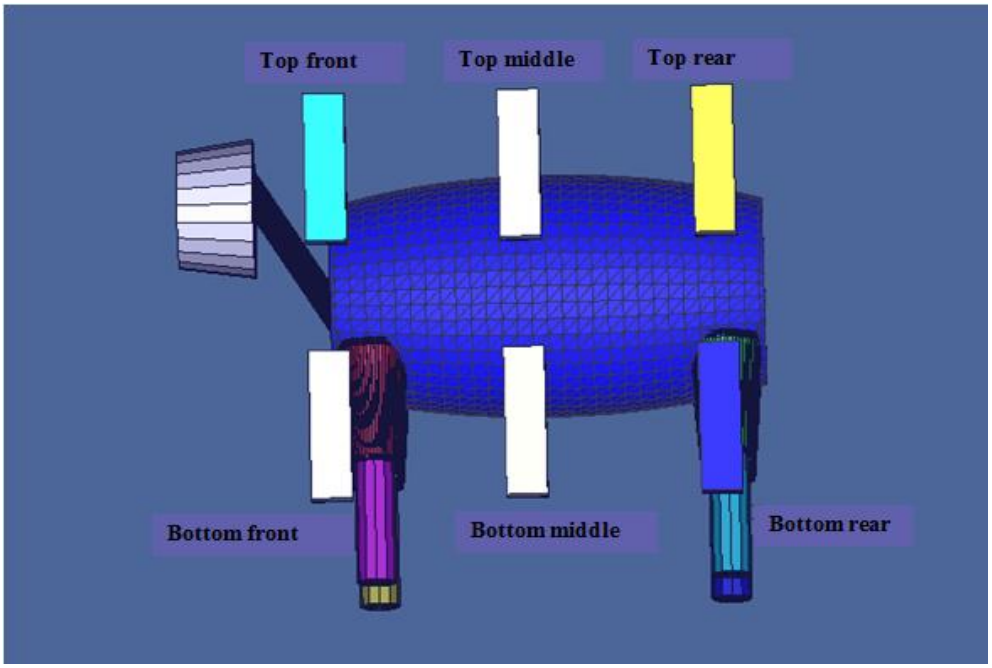

Fig. 10: Detectors placed perpendicular to the ground with the positions labeled.

After the point source simulation, a distributed source case was considered. To represent a distributed source, 20 point sources were spread across a square patch of 15.26 cm diagonal. The source positions were varied and the detector responses were collected. Orientations of the detectors were also changed as in the case of point source. The results were used to make a comparison of point source and distributed source response.

Next set of simulations included the cow and the cattle chute. Detector positions were not varied. Cow was positioned at the center. Response from the simulation was compared with the results when there was no chute. Texas A&M University Animal Science Department collaborators indicated that when a cow is made to enter the chute it always resists moving forward and stands at the back. So, a simulation was executed with the cow standing at the back of the chute and the detector position was changed such that two detectors were placed exactly aligning the center of the chute and the remaining four detectors were placed at the ends of the chute.

Yet another case was considered where the cow was positioned at the exit of the chute such that its head and neck region was outside of the chute. This case was taken because the hydraulic neck squeezers can be used to hold the cow. This restricts the forward or backward movement of the cow without causing undue stress to the animal. In this simulation, five detectors were used - four facing the main body and one facing the head.

Next, set of MCNP simulations were done with 2” ×4” ×4” detectors. Eight of these detectors were placed on one side of the cow. The orientations of detectors were

varied to see the changes in response and find the best orientation. Four different configurations were considered for the simulations. The count rate obtained in each case was compared with that obtained using 2" ×4" ×16" detectors. In each of the above cases MDAs were calculated.

A simulation with different radioactive sources representing the contamination on the cow was carried out and the MDA for each source was calculated. Here six detectors (2" ×4" ×16") were used and the cow was positioned at the back of the chute. This was done to check the effectiveness of the detector orientation in determining different radioisotopes of different energies. ^{241}Am, ^{133}Ba, ^{137}Cs, and ^{60}Co sources were used. These nuclides were used because they span a wide range of energy from 59 keV to 1172 keV.

II.G. Environmental Radiation Background Simulation

The background was simulated by modeling a 1 ft. deep concrete slab of width 5 m and length 5 m. the specific activities, the composition of the concrete and the radiation source term were collected from a previous work[24]. The total activity of the source was calculated using Eq. 6. MCNP runs were carried out with this background alone as the source of radiation. Appendix A has a representative MCNP input used in this work. The input has both background source term and the source representing contamination. The results obtained were used to calculate the MDA and signal to noise ratio. Appendix B has the list of nuclides, which were uniformly spread across the volume of the concrete slab, and their corresponding activities.

$$A_{tot} = m \sum_i S.A_i \quad (6)$$

Where A_{tot} is the total activity of the concrete slab;

m= mass of the concrete slab = density of concrete × volume of the slab

$S.A_i$ = specific activity of the i^{th} nuclide (radioactivity per unit mass of concrete).

II. H. Calculation of Minimum Detectable Activity (MDA)

MDA is a measure of sensitivity of a particular detection system or the lowest amount of radioactivity that can be detected by the system. The MDA for a system depends on the factors like the normal radiation background counts and the efficiency of the system itself.

To obtain MDA, the result from the simulation with ^{137}Cs source and the result from background simulation for the same configuration were used. The output from the ^{137}Cs source alone was used to calculate the efficiency of the detection system and the output of the background was used to determine the mean background count. Eq. 7 through 9 was used to calculate the MDA values[25].

$$\alpha_D = \frac{L_D}{K} \quad (7)$$

$$K = \in T \quad (8)$$

$$L_D = 2.71 + 4.65\sqrt{B} \quad (9)$$

Where α_D = MDA (dps or Ci),

LD = detection limit (counts),

$\in$=efficiency of the detector (cpɣ),

T = counting time (s) and

B = mean background count.

The constants in Eq. 9 were chosen such that there was 95 % confidence in saying the counts exist. The error associated with the MDA was calculated using Eq. 10.

$$\delta_{MDA} = MDA \times \left[\left(\frac{\delta_{L_D}}{L_D}\right)^2 + \left(\frac{\delta_\epsilon}{\epsilon}\right)^2\right]^{\frac{1}{2}} \quad (10)$$

Where, error associated with $L_D = \delta_{L_D} = \frac{2.325}{\sqrt{B}}\delta_B$,

δ_ϵ = error associated with efficiency (cpγ),

δ_B = error associated with the background count rate (cps).

There are several other factors that contribute to the natural background which were not considered in the simulation of the background radiation source:

a. Cosmic rays: The interaction of cosmic rays with various elements found in the atmosphere contributes to the natural background.
b. Skyshine: Gamma rays from the ground which move upwards can be scattered back by the molecules in the atmosphere contributing to the natural background. Skyshine will result in addition of 20 % of the natural background counts.
c. Radiation from the cow: All animals will have a certain level of radioactivity in its body mainly due to K-40.
d. Radiation from the ground: The concrete slab modeled was just 25 m^2 area which is very small. The actual contribution to the background comes from a much larger area of the ground.

These sources of background will affect the MDA values calculated and also influence the performance of the portal monitor. Therefore all MDA values

presented in this thesis are valid for the configuration that was considered while simulating the background radiation source.

CHAPTER III

RESULTS AND DISCUSSIONS

III.A. Point Source – Parallel vs. Perpendicular Orientation of the Detector

First simulations were carried out with a point source on the abdominal region of the cow. 2”×4”×16” detectors were placed 6 inches away from the cow model. The orientations of the detectors were as shown in Fig.9. The source is positioned such that it was near to the rear middle detector and F8 tally results were collected. As mentioned earlier, F8 tally results are normalized per starting particle and when multiplied with the activity of the source and branching ratio gives the count rate. The F8 tally (pulse height tally) definition was written such that the count rates at the 6 detectors were obtained in the MCNP simulation output. The plot shown in Fig. 11 illustrates the energy spectrum collected by the NaI detectors. The source position was then changed to another position to collect the spectrum which is demonstrated in Fig. 12. This time the source was positioned near to the front middle detector. Fig.11 and Fig. 12 show that the counts registered in the detector near to the source was higher than that in the other detectors as expected. This means, individual response of the detectors can give details of the source location. For example, the spectrum shown in Fig.11 shows that the source was located in the region near to the rear middle detector. The source position was changed and 5 more simulations were made and the spectra were collected. The detector positions were not altered in these runs.

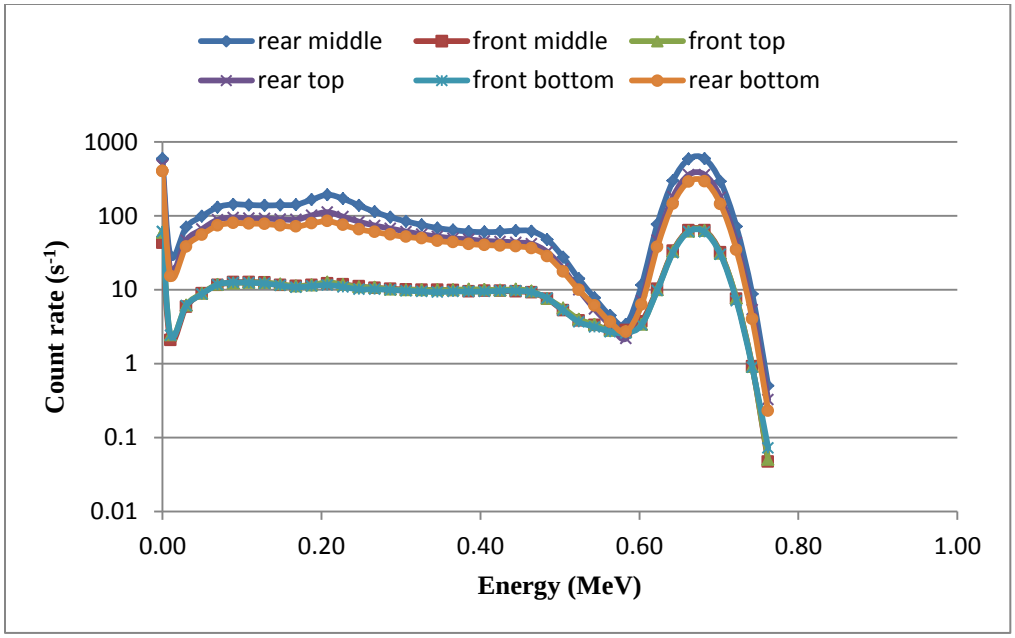

Fig. 11: Spectrum obtained for the point source case where the source was placed near to the rear middle detector.

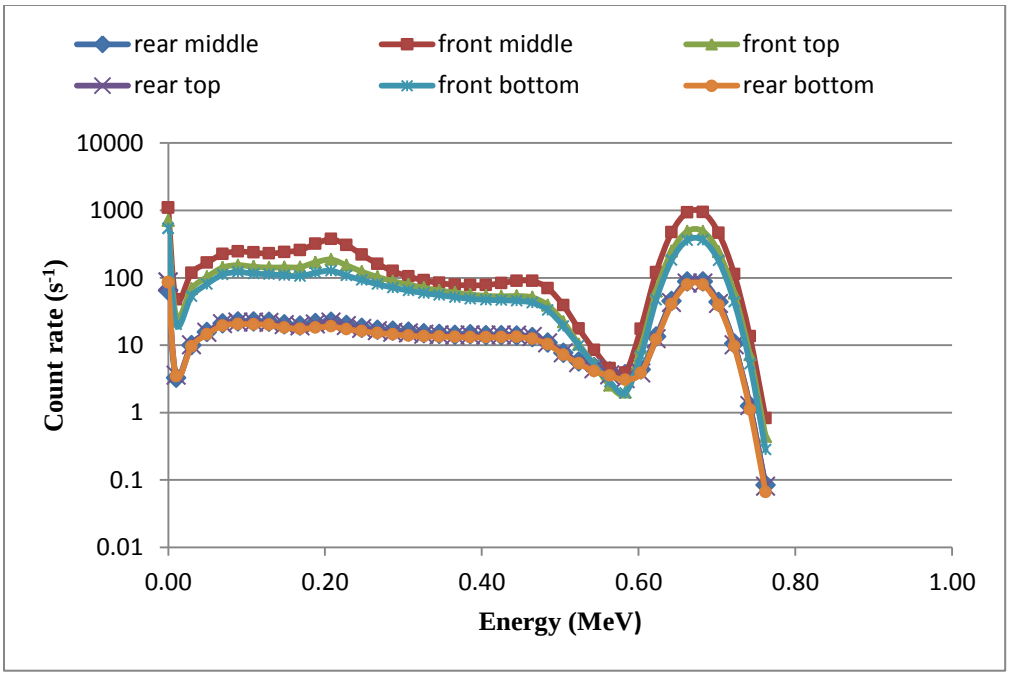

Fig. 12: Spectrum obtained in the case where point source was placed near to the front middle detector.

Detector positions and orientations were changed such that the 2”×16” face was perpendicular to the ground as shown in Fig. 10. MCNP simulations for the source positions as in Fig. 11 were carried out and the spectra were collected. Fig. 13 and 14 show the spectra obtained for the case where the source was placed on the surface of the cow at the same positions used in the previous cases. Considering the parallel and perpendicular cases, a few observations are made:

- In the case of parallel orientation of the detectors:
  - The counts registered in each of the 3 detectors placed at the rear side did not differ much when the source was near to the front side detectors.
  - Same is true for the detectors placed in the front side when the source was near to the rear side detectors.
- In the case of Perpendicular orientation of the detectors:
  - The counts registered in each detector show a difference.
  - This will actually assist in localizing the source position.

Hence, perpendicular orientation is preferred because of its ability to estimate the location of the source.

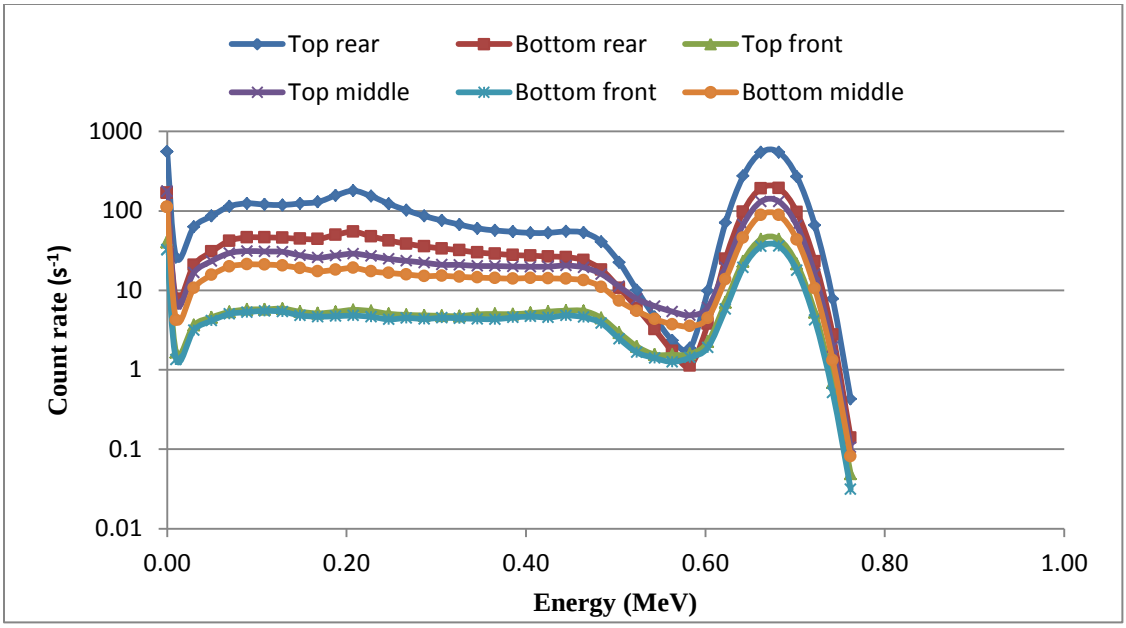

Fig. 13: Spectrum obtained in the case where the detectors were placed perpendicular to the ground and the source placed at the position as in Fig. 11 case

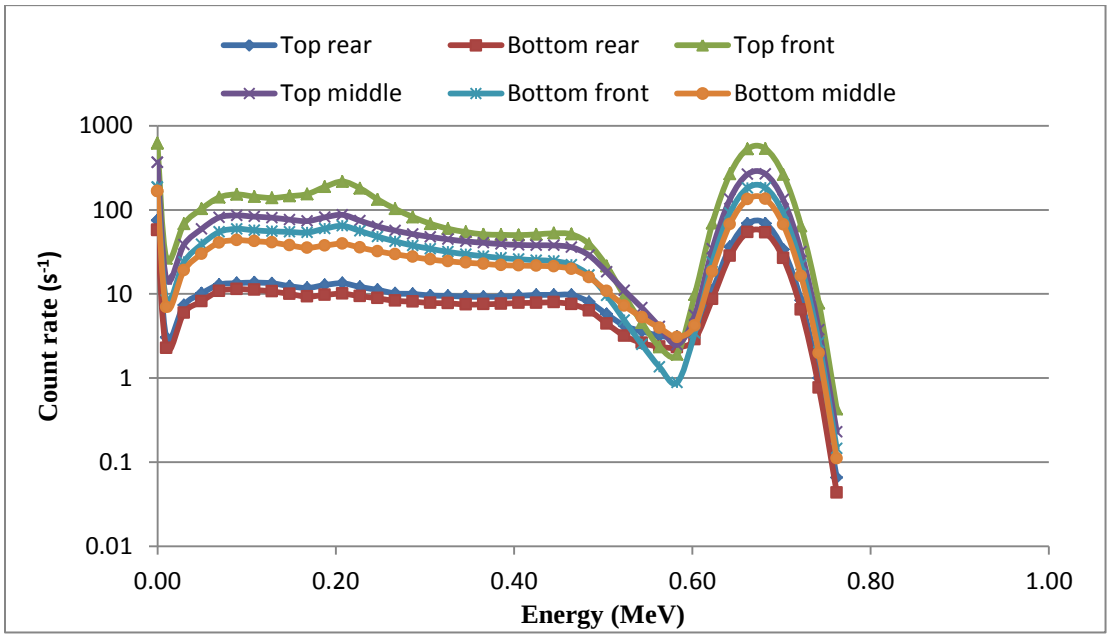

Fig. 14: Spectrum obtained in the case where the detectors were placed perpendicular to the ground and the source placed at the position as in Fig. 12 case

A comparison was made between the spectrum obtained for the cases of parallel and perpendicular orientation of the detectors to see the difference in the counts getting registered. The source was placed at the center of belly region. Fig. 15 is the spectrum comparison of the two cases. Here, the perpendicular orientation of the detectors registered more number of counts. The count rates obtained for different source positions are listed in Table IV. The negative sign on the percent difference value means that the count rate obtained in the case of parallel orientation of the detectors is smaller than that of perpendicular orientation. Fig. 16 is the histogram of the total count rate registered in the detectors for the parallel and perpendicular cases and various source positions. The count rate in the perpendicular case is higher for the source positions on belly and nose, while it is high in parallel case when the source is on the detector side. This means that the perpendicular orientation has better coverage of the cow's body surface, which is not directly facing the detector. Surface near the nose is a very sensitive region to be considered because any contamination on nose may indicate internal contamination. Once the cow is contaminated internally, it becomes unfit to enter the food chain. So, it is important that the contamination near nose be detected. This is another reason to choose perpendicular orientation over parallel.

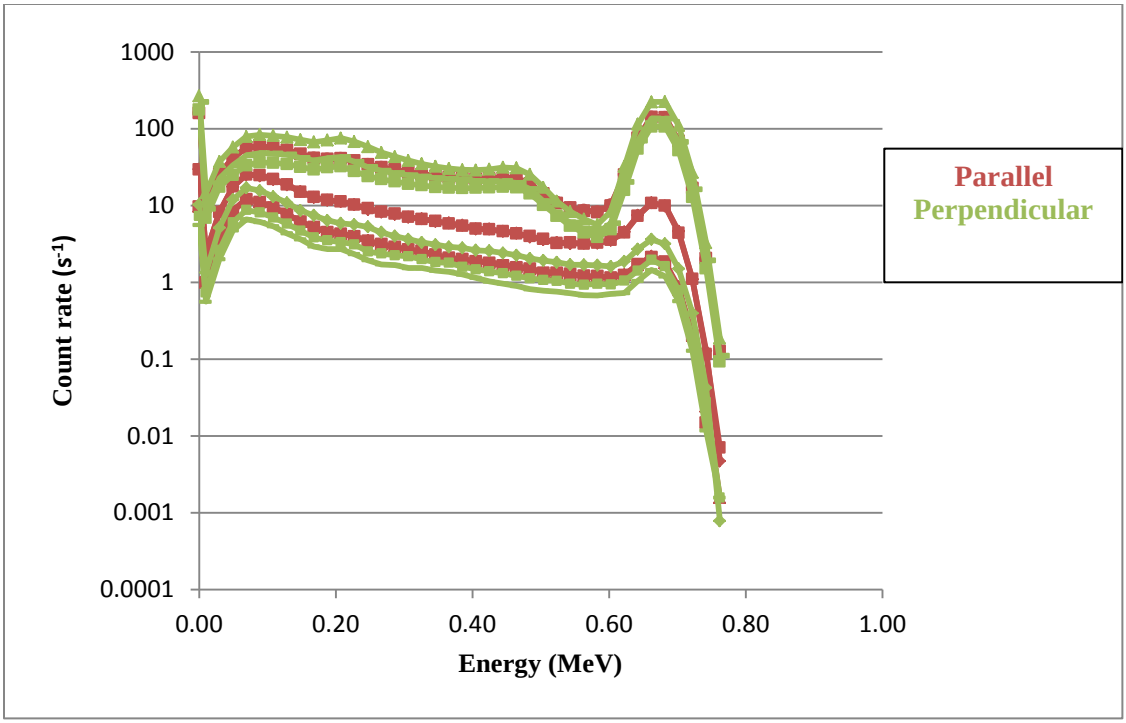

Fig. 15: Comparison of the spectrum with detectors placed parallel and perpendicular to the ground for a point source on belly.

TABLE IV

Total count rate registered for different point source positions.

Source Position	**Count Rate (s^{-1})**		**Percent difference**
	Parallel	**perpendicular**	
Rear detector side	4779.6±2.7	3478.6±2.3	31.5
Front detector side	6771.1±2.3	4133.9±1.8	48.4
On the belly	1120.4±0.9	1620.6±1.1	-36.5
On the nose	146.8±0.3	259.7±0.5	-55.6

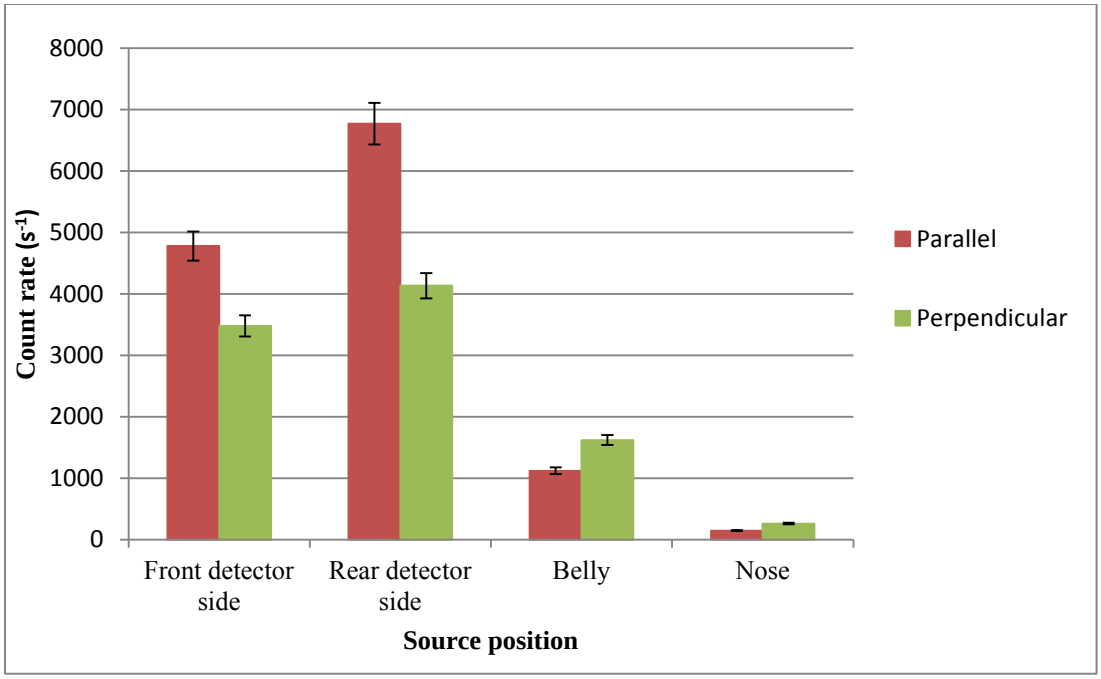

Fig. 16: Histogram of the total count rate recorded in the detectors in the parallel and perpendicular orientation of the detectors.

III.B. Distributed Source – Parallel vs. Perpendicular Orientation of the Detector

MCNP simulations were made with the same number and orientation of the detectors used for point source cases, but now the sources were distributed. First the detectors were kept parallel to the ground, the distributed sources were positioned at the center of the belly region and spectrum was collected. Then the source positions were varied and spectra were collected in each case. The procedure followed with the point source was repeated. A comparison of parallel and perpendicular positions of the detector is presented in Fig. 17. The spectrum obtained in the case of detectors placed perpendicular to the ground showed higher count rate as compared to the case where detectors placed parallel to the ground. The count rate obtained for 4 different positions

are tabulated in Table V. The negative signs on the percent difference column indicate that the count rate obtained for the parallel case is lower than the perpendicular case.

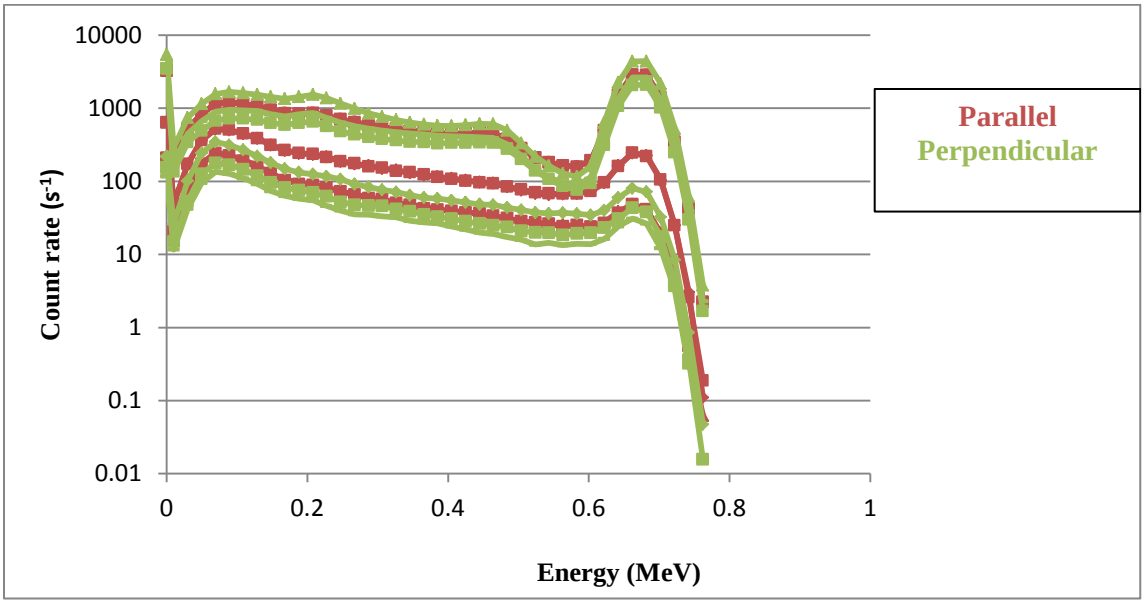

Fig. 17: A comparison of the spectra obtained with parallel and perpendicular orientation of the detector with distributed source on the belly region.

TABLE V

Total count rate registered for different distributed source positions.

Source position	**Count Rate (s^{-1})**		**Percent difference**
	Parallel	**Perpendicular**	
Belly	19137.4±19.0	26522.3±22.5	-32.3
Top (Loin)	16945.9±14.7	18567.8±16.9	-9.1
Side near the detector	135685.6±104.4	75565.6±62.0	56.9
Side away from the detector	493.9±4.2	455.7±4.1	8.0

The count rate obtained is again higher for parallel case where the source was located on the region facing the detector. From the comparison of parallel to perpendicular placement of detectors, it was clear that perpendicular orientation of the detectors is more sensitive than the parallel orientation in detecting sources located on the belly, loin and nose. So for all future work perpendicular orientation was considered.

III.C. Point Source vs. Distributed Source

The spectrum from the distributed source looks similar to that obtained in the case of point source except that the counts recorded in the distributed source case was higher. This was expected because the activity of the distributed source is much higher than the point source. Fig. 18 shows the difference between the spectrum for point source and distributed source.

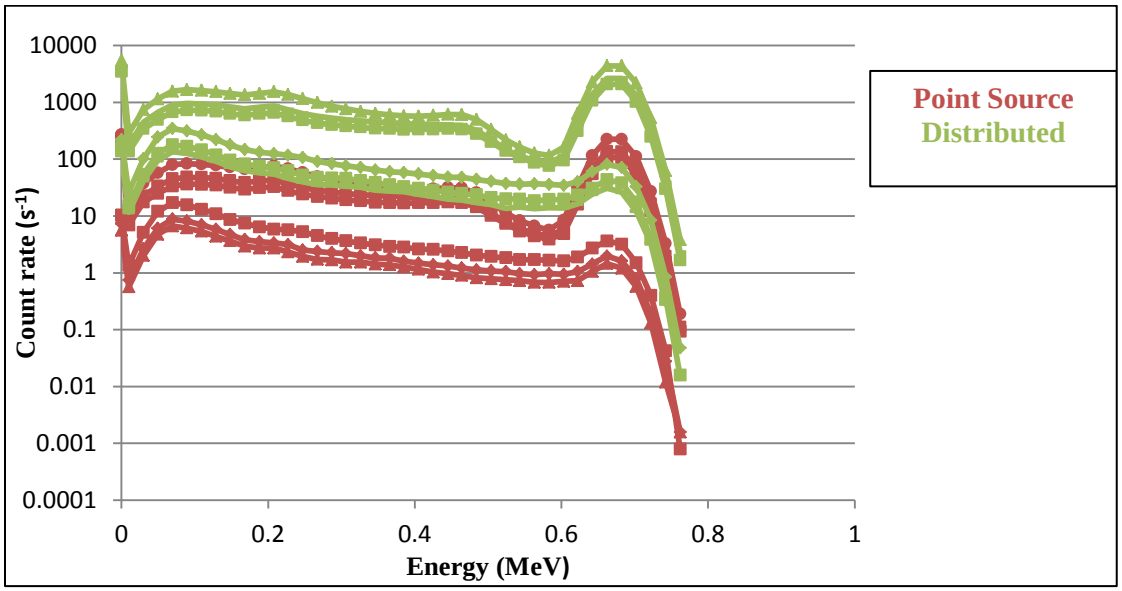

Fig. 18: A comparison of the spectra obtained for point and distributed source on the belly region.

III.D. With and Without Cattle Chute

MCNP simulations were performed with the cattle chute for both point and distributed case. The detectors were oriented in the perpendicular direction. The results obtained were similar to that obtained without the chute. A comparison of the two is shown in Fig. 19. The count rate obtained without chute was 1618 cps and that with chute 1315 cps. This means the count rate without chute was 1.2 times higher than the case where the chute was not present. The presence of the metal bars caused the count rate to decrease by ~19%. Fig. 20 demonstrates the difference in the total count rate.

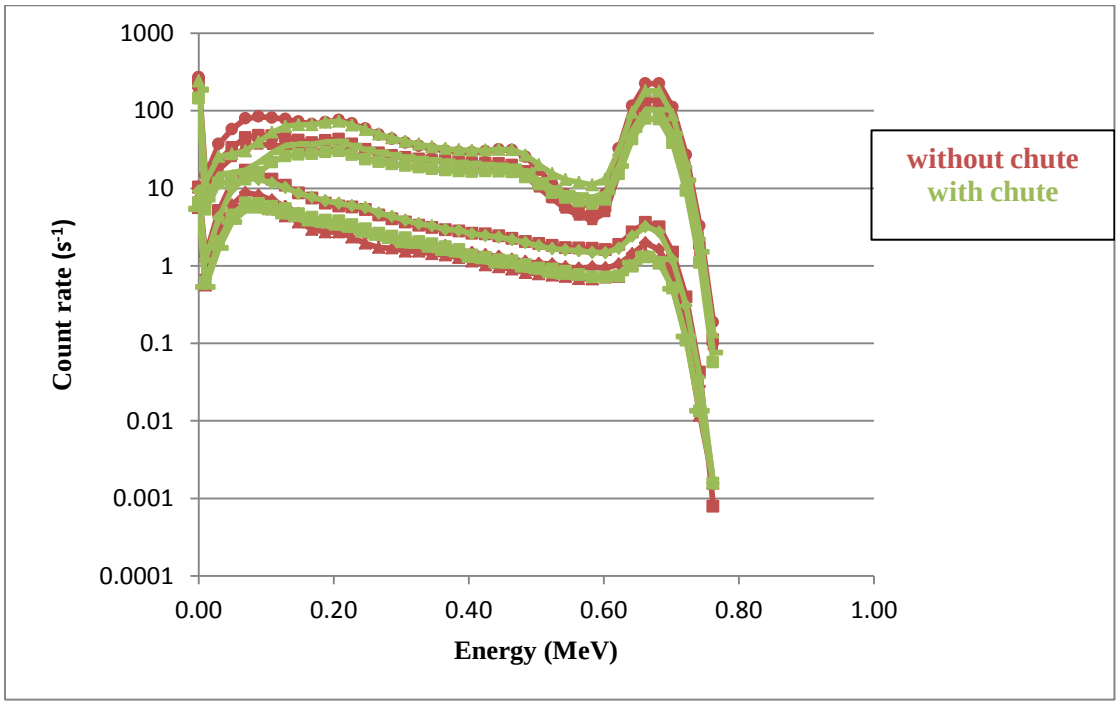

Fig. 19: The comparison of the spectrum obtained with and without chute and with a point source on the belly region.

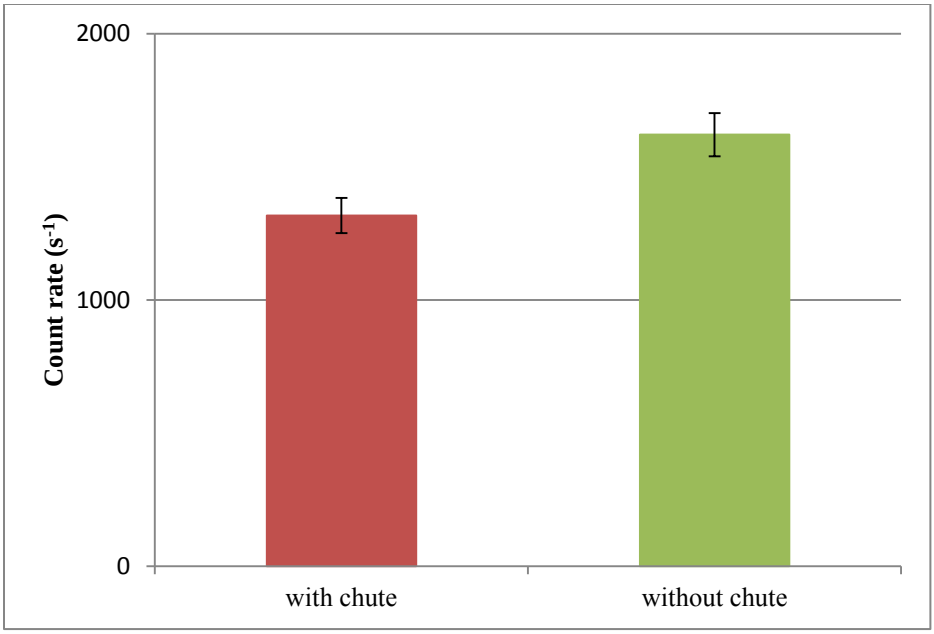

Fig. 20: Histogram showing the count rate obtained for the case with chute and without chute.

III.E. Six Detectors vs. Five Detectors

Real contamination on a cow could be anywhere. Therefore choosing the best placement and orientation of detectors is essential. Detectors should be oriented such that they can detect the source of contamination effectively, potentially identify the radionuclide and also be able to estimate the location. For this purpose, two cow positions were considered. First, the cow was made to stand at the entrance of the chute (representing the situation where the cow is resisting to move forward) and the detectors were spread apart such that 2 detectors were positioned exactly at the center of the chute and the other 4 were placed at the ends. The detector orientation and the cow's position are shown in Fig. 21. Second, the cow was made to stand at the front portion of the chute

where its neck can be secured using hydraulic squeezer without causing undue stress to the animal. In this case five detectors were used as shown in Fig. 22.

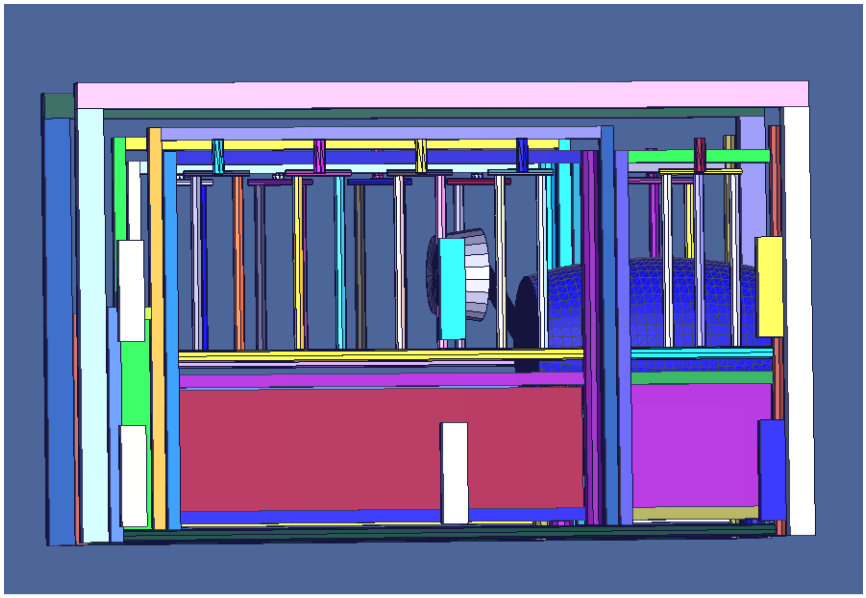

Fig. 21: Cow is standing at the entrance of the chute and the detectors are spread apart.

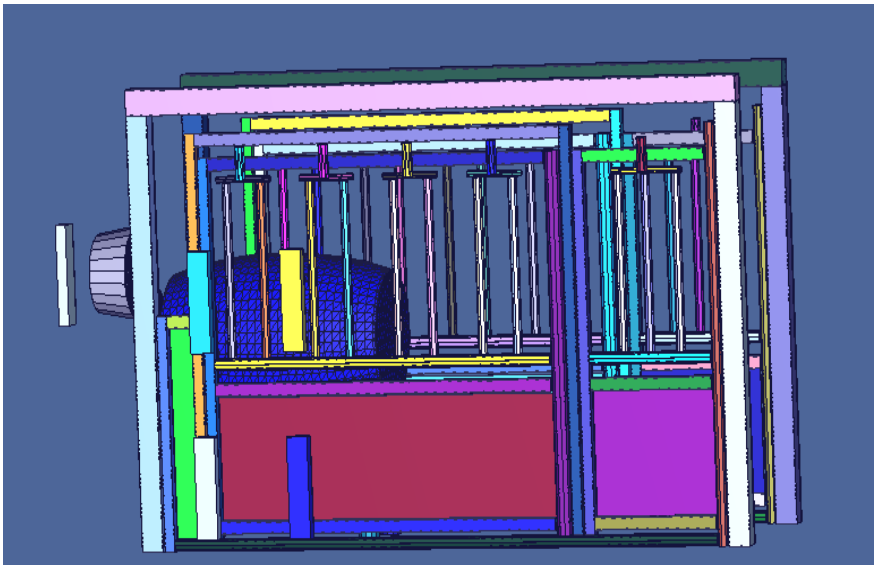

Fig. 22: Cow is at the exit and one detector is placed in-front of the head and other detectors are placed on the sides.

MCNP simulations were performed and the results are shown in Fig. 23. This figure compares the spectrum obtained in these two cases when the source was placed on the nose region. The five detector case has the advantage over the six detectors case because the cow is made to stand still as a result of which the detectors response can be used directly to estimate the location of the source. Also, this orientation gives better identification if the contamination is near the nose region. The count rate registered in the detector close to the head was 5501 cps in five detectors case and 641 cps in six detectors case. However, this orientation has a limitation. The Animal Science Department collaborators pointed out that it takes around 10 s to move the cow through the chute and then securing it using the hydraulic squeezers. Whereas allowing the animal move through without interruption would consume much less time (Dr. Andy Herring, personal communication, February, 2011). The time mentioned may seem tiny but scanning nearly 50,000 cattle at a feedlot must be done in a time efficient manner. Also, every time the animal is scanned the detector in front of the head of the cow has to be displaced in-order to let the animal move forward. Hence, six detectors were preferred.

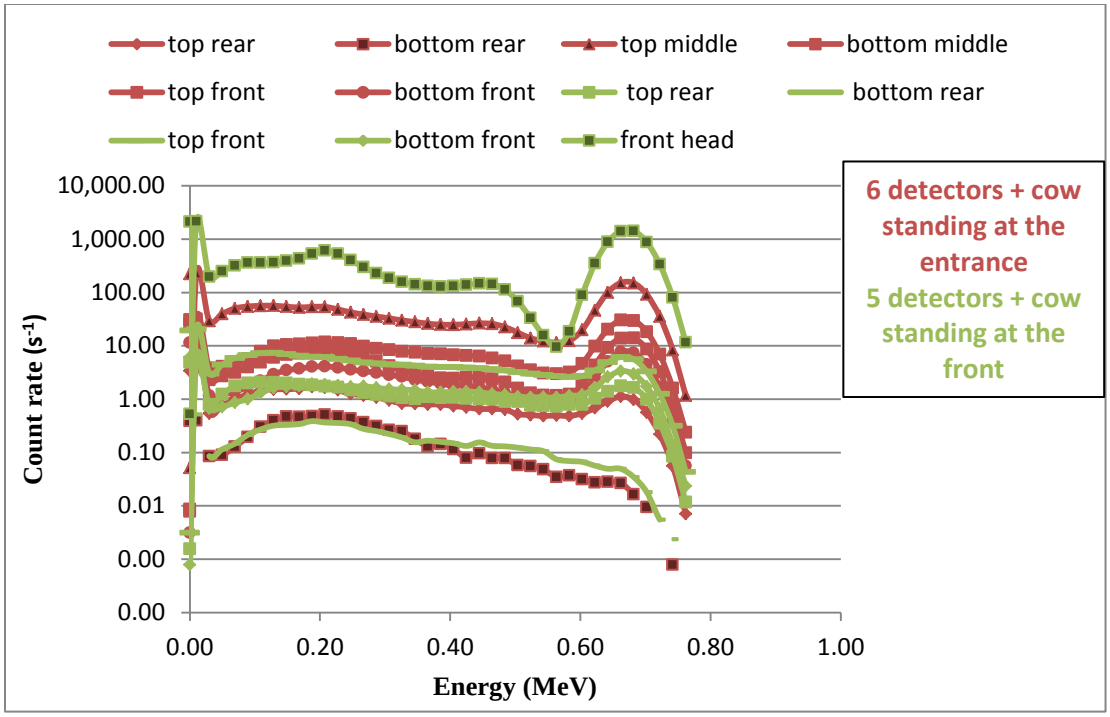

Fig. 23: A comparison of the spectra with six and five detectors with the source positioned on the nose.

III.F. Different Orientations of Eight 2"×4"×4" Detectors and its Corresponding MDA Values Compared with Six 2"×4"×16" Detectors

In the next set of simulations, 8 (2"x4" x4") detectors were used. Placement of detectors was varied without changing the source positions and position of the cow. Source was placed on the belly of the cow and the different detector orientations are shown in Fig. 24.

- In configuration 1, the placement of the 6 (2"×4"×16") detectors are shown.
- In configuration 2, 8 detectors were positioned such that 4 detectors were placed on top to cover any contamination on the head and loin region and the other 4 were placed below to detect contamination on the belly and legs.

- In configuration 3, the detector placement was similar to that of Configuration 2 but now the top and bottom detector pairs were in line with each other.
- In Configuration 4, the detectors were arranged in 3 rows so that it covered the head region abdominal region and near the legs. The top row had 2 detectors, mid row had 4 detectors and bottom row had 2 detectors.
- In configuration 5, again detectors were in 3 rows. Top row consisted of 3 detectors, mid row with 2 detectors and the bottom with 3 detectors.

The spectral results obtained with these configurations were compared. Table VI shows the results of the counts registered in the 662 keV gamma peak region. It is clear that the 2"×4"×16" detectors registered (10485 cps) nearly 3 times higher count rate as compared to 2"×4"×4" detectors. It should be noted here that the total area of the 6 2"×4"×16" detectors exposed to the source was 3 times higher than 8 2"×4"×4" detectors. In each case, a simulation was made to collect the background counts registered in the detectors. The background count was used to calculate the MDA of the detector system. The values of the MDA in μCi are tabulated in Table VII. These values of MDA correspond to ^{137}Cs nuclide.

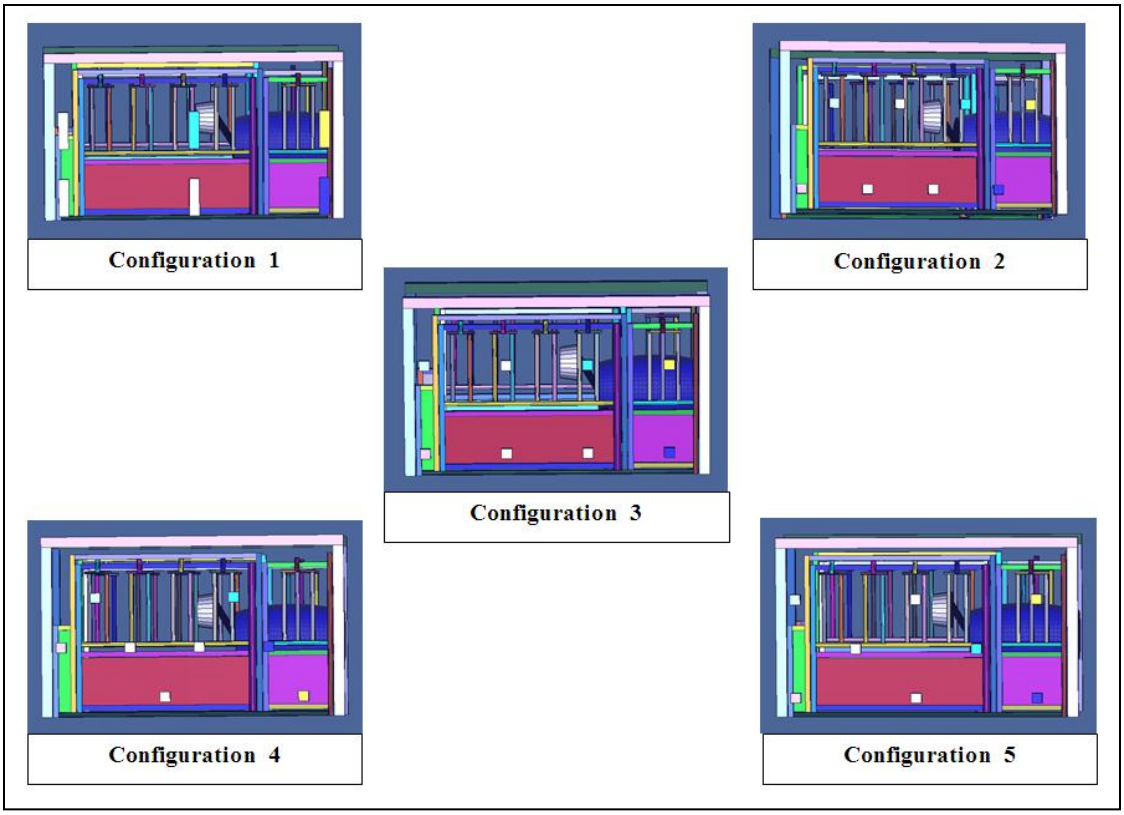

Fig. 24: Different orientation of the detectors used to find the optimal configuration.

TABLE VI

Total counts registered in the detectors for different orientation of detectors.

Orientation	**Total Counts registered in the detectors (s^{-1})**
Configuration 1 (2”×4”×16”)	10485±12.8
Configuration 2 (2”×4”×4”)	3306±7.2
Configuration 3 (2”×4”×4”)	3932±7.9
Configuration 4 (2”×4”×4”)	3102±7.0
Configuration 5 (2”×4”×4”)	3019±6.9

TABLE VII

Calculated MDA values for different array of detector set up for 1 s.

Orientation	**Background Count rate (cps)**	**Efficiency of the detection system (Counts per ɣ) $\times 10^{-4}$**	**Efficiency (counts per ɣ per cm^3) $\times 10^{-7}$**	**Limit of Detection, L_D (cps)**	**MDA (μCi)**
Configuration 1 (2”×4”×16”)	75.3±0.4	33.34±0.04	2.649±0.003	43.06±0.11	0.411±0.0012
Configuration 2 (2”×4”×4”)	27.8±0.3	10.51±0.02	2.505±0.005	27.23±0.11	0.824±0.0039
Configuration 3 (2”×4”×4”)	27.3±0.3	12.5±0.03	2.980±0.006	27.01±0.12	0.687±0.0032
Configuration 4 (2”×4”×4”)	27.1±0.3	9.87±0.02	2.353±0.005	26.92±0.12	0.867±0.0042
Configuration 5 (2”×4”×4”)	27.6±0.3	9.60±0.02	2.288±0.005	27.14±0.12	0.899±0.0043

The MDA value is lowest for configuration 1 as compared to other configurations because the efficiency of the 6 detector system is highest. The MDA implies that using 6 detector system, contamination as low as 0.4 μCi can be detected with 95% confidence. In this case, since the source was on belly, the detector responses on either side will be symmetrical. So, it can be assumed that the efficiency of 12 detectors system is double the value obtained with 6 detectors. Hence, the MDA value decreases by a factor of 2. This is not true for other source positions because the

radiation will be shielded by different amounts for different source location. The MDA values obtained for other configurations are much smaller as compared to that of configuration 1. The efficiency per unit volume is also presented. Since configuration 1 had the lowest MDA and also the efficiency per unit volume remained almost the same, configuration 1 was chosen for the prototype build. Also it provided the lowest MDA. Furthermore, in order to achieve a 0.4 μCi MDA using 2"x4"x4" detectors, more number of detectors are needed and electronic peripherals would have to be purchased. This was not within the project budget.

III.G. Multiple Sources and MDA Values for Different Nuclides

To know the MDA values for different sources of contamination, MCNP simulation was carried out with the ^{137}Cs source replaced by ^{241}Am, ^{133}Ba, ^{137}Cs, ^{60}Co sources. In each case, the MDA was calculated and the results are tabulated in Table VIII. Fig. 25 shows the spectrum collected by the bottom rear detector for these 4 distributed sources placed on the belly. The efficiency of the system decreased as energy of the source increased. This is because higher energy radiation would pass through the detector material without depositing its energy. However, the efficiency of the system for ^{241}Am nuclide was much lower because the energy was low so that most of the gammas did not make it to the detectors. To calculate the MDA value for specific nuclides the MDA value obtained using Eq. 1 was divided by the branching ratio of the corresponding energy which yielded the final MDA value. This value remained almost the same for all the tested nuclide energies, except for ^{241}Am gamma energy of 59.5keV.

TABLE VIII

MDA values calculated for different nuclides.

Radion uclide	Energy (keV)	Background Count rate (cps)	Limit of Detection, L_D (cps)	Efficiency (counts per ɣ)	MDA (µCi)
^{241}Am	59.5	49.3±0.3	35.35±0.11	1.05±0.007	25.43±0.19
^{133}Ba	356	103±0.5	49.91±0.11	49.04±0.05	0.443±0.0011
^{137}Cs	662	75.6±0.4	42.06±0.11	34.45±0.04	0.411±0.0012
^{60}Co	1172	16.4±0.2	21.54±0.11	12.21±0.003	0.477±0.0025
^{60}Co	1332	8.7±0.1	16.39±0.11	10.29±0.003	0.431±0.0029

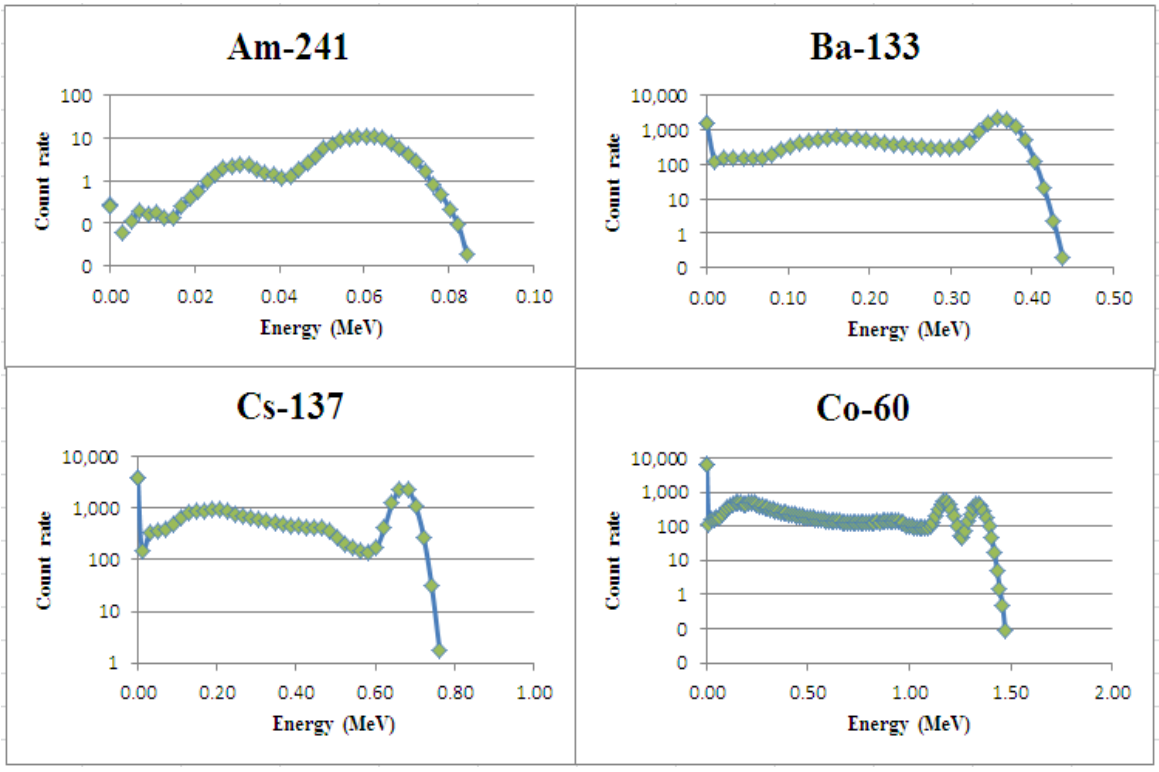

Fig. 25: Spectrum obtained with different sources on the cow.

To study the dependence of MDA values with the source positions, MDA was calculated for different source positions. The results are tabulated in Table IX. The values obtained suggest that the contamination of much lower activity (~0.2 μCi) can be determined if it is on the nose or the side regions as compared to belly region. This is because the sources on the nose and side regions were closer to the detectors. The MDA for point and distributed source were also considered and the results are tabulated in Table IX. The values obtained were the same for point and distributed source. Here the source positions in both the cases were on the belly region. So the efficiency of the system remained almost the same and hence the MDA value remained the same.

TABLE IX

MDA values for various source positions and for distributed source.

Source position	**Background (cps)**	**Limit of detection L_D (cps)**	**Efficiency (counts per γ) $\times 10^{-4}$**	**MDA(μCi)**
On the belly	75.6±0.4	43.14±0.11	34.45±0.04	0.398±0.0011
Side near to the rear detector	75.6±0.4	43.14±0.11	60.36±0.05	0.227±0.0006
On the nose	75.6±0.4	43.14±0.11	55.36±0.05	0.248±0.0007
Point source on the belly	75.6±0.4	43.14±0.11	34.45±0.04	0.398±0.0011
Distributed source on the belly	75.6±0.4	43.14±0.11	33.04±0.04	0.411±0.0012

CHAPTER IV

SUMMARY AND CONCLUSIONS

A radiological accident may result in the contamination of surrounding places, people, animals, vegetation etc. It is important to consider decontamination of cattle in such a situation. The USDA has the responsibility of evaluating and decontaminating the animals. This thesis work was funded by USDA to develop a gamma radiation portal monitor which can be used for scanning livestock. The work was carried out using MCNP radiation transport code. A cow, cattle chute and detectors were modeled and simulations were carried out to know the optimal detector configuration. NaI detectors were modeled in this work because of its ability to identify the radionuclides. Also, it is inexpensive as comapared to HPGe detectors. MCNP simulations were performed for different source placements, detector placements and size. Also, the MDA for different configurations were calculated.

The results from the MCNP for a point source case with 6 (2”×4”×16”) detectors 6 inches away from the source suggested that the detector close to the source picked up more number of counts. A comparison of the spectra from parallel and perpendicular cases showed the perpendicular orientation was better in estimating the source location. Also, the perpendicular orientation registered high count rate for source location on the nose which is a crucial part. Contamination on the nose would suggest possible internal contamination. Due to this reason perpendicular orientation was preferred for all further

simulations. The detector system was tested by simulating a distributed source and the results were similar to that of the point source case.

In order to protect the animals and the detector system from any kind of damage a cattle chute was necessary and hence was included in the model. The procedure that was followed without chute was now repeated with chute. The count rate obtained in this situation reduced by ~19 % because of the presence of the metallic chute which acted as a shield. Two extreme cases were considered for the next simulation which included cow standing at the back of the chute and cow standing at the front. In the former case, six detectors were used and the later case consisted of five detectors. The five detector configuration provided better identification of contamination near the nose region. However, this configuration had a disadvantage in which the detector infront of the head was to be moved everytime an animal scanned.

The 6 detector configuration results were then compared with that of 8 (2"×4"×4") detectors placed in different configurations. The count rate in the 6 detectors were nearly 3 times higher than that of 8 smaller detectors. The MDA values for each configuration was calculated. The 6 detector configuration had a MDA value of 0.411 μCi for a scan noramlized to one second time and for ^{137}Cs source. The other configuration had MDA values ranging from 0.6 – 0.9 μCi. The MDA values for different sources were also calculated. The value remained almost the same for energies ranging from 356 keV (of ^{133}Ba) to 1332 keV (of ^{60}Co). For 59.5 keV energy of ^{241}Am the MDA value was 25.43 μCi. The MDA values were determined for different source locations. It was 0.248 μCi for source location near the nose. However these MDA

values are valid for the configuration simulated for this particular work and is subject to change if different background sources are considered.

Also, the portal designed in this work can be used for scanning cattle of varying size but not for smaller animals like sheep. The detectors used in this work are large which makes it difficult to use it to scan small animals because it will not be helpful in determining the location of contamination. For small animals, using smaller detectors could more efficiently determine source location.

In conclusion, this work was able to determine the optimal configuration for determining external contamination on cattle. The MDA value indicated for this configuration is the best possible MDA value. However, in real life this value will be higher because the background inludes radiation from much larger area of the ground than that is considered in the work. Also other natural sources like cosmic rays, skyshine and radiation from the cow contributes to the background.

IV.A. Future Work

Future work in this might include simulating all possible sources of background and evaluate a more precise MDA value. Also compartmental model of cow can be developed to determine the contamination in different organs in the case of internal contamination.

Other works include testing of the portal monitor developed for its performance on field. A practical MDA value should be determined and its ability to determine

location and level of contamination should be tested. The performance of this portal should be compared with existing human portals.

REFERENCES

1. S. COREN, "The Dogs of Hurricane Katrina": http://www.moderndogmagazine.com/articles/dogs-hurricane-katrina/151 (*Last accessed: Jan 2012*).
2. OTTO, DAN and J. D. LAWRENCE, "Economic Impact of the United States Beef Industry", Iowa State University, Department of Economics, 2001.
3. "2007 Census of Agriculture", USDA, Vol. 1, *Geographic Area Series*, Part 51, December 2009. http://www.agcensus.usda.gov/Publications/2007/Full_Report/usv1.pdf (*Last accessed: Jan 2012*).
4. "U.S. Beef and Cattle Industry: Background Statistics and Information", USDA http://www.ers.usda.gov/news/BSECoverage.htm (*Last accessed: Jan 2012*).
5. National Response Framework, Homeland Security, Jan 2008 www.fema.gov/pdf/emergency/nrf/nrf-core.pdf (*Last accessed Jan 2012*).
6. Nuclear/Radiological Incident Annex, June 2008: http://www.fema.gov/pdf/emergency/nrf/nrf_nuclearradiologicalincidentannex.pdf (*Last accessed October 2011*).
7. "Determining Lower Limit of Detection and Minimum Detectable Activity for Radiation Measurements", USDA, Radiation Safety Program, Technical bulletin. http://www.rss.usda.gov/publications/mdatb.htm (*Last accessed: Jan 2012*).
8. C. M. MARIANNO, "Pet Monitoring During a Radiological Emergency", *National Radiological Preparedness Conference*, April 2008.

9. X-5 MONTE CARLO TEAM, "MCNP — A General Monte Carlo N-Particle Transport Code", Version 5, Vol. 1 & 2, LANL, April 2003.

10. J. SEVERA and J. BAR, *Handbook of Radioactive Contamination and Decontamination*, Elsevier Science Publishing Company, 1991.

11. "Extensive Testing on Surrogate Skin Indicates RDS's Mass Effect Solutions Effective for Skin Radiation Decontamination", Radiation Decontamination Solutions, LLC., http://www.raddecon.com/news.htm (*Last accessed Jan 2012*)

12. G. F. KNOLL, *Radiation Detection and Measurement*, John Wiley & Sons, 1979.

13. P. E. FEHLAU, *An Application Guide to Pedestrian SNM Monitors*, LANL, 1986.

14. D.C. STROMSWOLD, E.R. SICILIANO, J.E. SCHWEPPE, J.H. ELY, B.D. MILBRATH, R.T. KOUZES, B.F. GEELHOOD. *Comparison of Plastic and NaI(Tl) Scintillators for Vehicle Portal Monitor Applications*, Nuclear Science Symposium Conference Record, **2**, 1065-1069 (2003).

15. K.C. TSOU, "Evaluation of Organometallic Compounds for Gamma Detection in Plastic Scintillators", *IEEE Transactions on Nuclear Science*, **12**, 28-33 (1965).

16. B. L. RUPERT, N. J. CHEREPY, B.W. STURM, R. D. SANNER and S. A. PAYNE, "Bismuth-Loaded Plastic Scintillators for Gamma-Ray Spectroscopy", *EPL*, **97**, 22002 (2012).

17. G. GILMORE, *Practical Gamma-Ray Spectrometry*, 2nd edition, John Wiley & sons, 2008.

18. H. A. SMITH, Jr., and M. LUCAS, *Passive Nondestructive Assay for Nuclear Materials: Gamma Ray Detectors*, LANL, 1991.

19. "Accidental Radioactive Contamination of Human Food and Animal Feeds": Recommendations for state & local government, 1998. http://www.fda.gov/downloads/MedicalDevices/DeviceRegulationandGuidance/GuidanceDocuments/UCM094513.pdf (*Last accessed Jan 2012*).

20. P. A. KARAM: "Radiological Terrorism, Human and Ecological Risk Assessment": *An International Journal*, **11**, 501-523 (2005).

21. M. W DENNY, *Air and Water: the Biology and Physics of Life's Media*, Princeton University Press, 1993.

22. J. R. YOUNG, *The Elements of Analytical Geometry: Comprehending the Doctrine of the Conic Sections, and the General Theory of Curves and Surfaces of the Second Order*, Harvard University, 1830.

23. N. P. BALI, N. CH. N. IYENGAR, *Text Book of Engineering Mathematics*, Laxmi Publications, 2004.

24. C. M. RYAN, "Determining the Impact of Concrete Roadways on Gamma Ray Background Readings for Radiation Portal Monitoring Systems", Master's Thesis, Texas A&M University, May 2011

25. L. A. CURRIE**, "**Limits for Qualitative Detection and Quantitative Determination. Application to Radiochemistry", *Anal. Chem*., **40**, 586–593 (1968).

APPENDIX A

```
c MCNP input for the background simulation
c ----cell cards------
  301 7 -2.301 -701
  302 7 -2.301 -702
  303 7 -2.301 -703
   1    1  -0.915 -1 -2 3 (6 :-7 :8 )(9 :-7 :8 )(10 :-7 :8 )          $ellipsoid
        (11 :-7 :8 )(19 :2 :-3 )(37 :-38 :-23 :24 )(21 :-22 :-25 :26 )
        (21 :-22 :-27 :28 )(21 :-22 :-29 :30 )(21 :-22 :-31 :32 )
        (21 :-22 :-33 :34 )(21 :-22 :-35 :36 )(46 :-47 :125 :-126 )
        (45 :-46 :127 :-128 )(44 :-45 :129 :-130 )(43 :-44 :131 :-132 )
        (41 :-42 :133 :-134 )(39 :-40 :135 :-136 )(-138 :139 :48 :-49 :50
         :-51 )(140 :-141 :48 :-49 :50 :-51 )
   2    1  -0.915 4 2 -5 (20 :-2 :5 )                                 $oblique cone/neck
   3    1  -0.915 -6 7 -8 (21 :-22 :125 :-126 )(12 :-7 :8 )           $cone/leg
   4    1  -0.915 -9 7 -8 (21 :-22 :-25 :26 )(13 :-7 :8 )             $cone/leg
   5    1  -0.915 -10 7 -8 (21 :-22 :-25 :26 )(14 :-7 :8 )            $cone/leg
   6    1  -0.915 -11 7 -8 (21 :-22 :125 :-126 )(15 :-7 :8 )          $cone/leg
   7    2   -2.06 -12 -7 16                          $cylinder lower leg
   8    2   -2.06 -13 -7 16                          $cylinder lower leg
   9    2   -2.06 -14 -7 16                          $cylinder lower leg
  10    2   -2.06 -15 -7 16                          $cylinder lower leg
  11    1  -0.915 -17 -18 5                          $cone/head
  12    2   -2.06 -19 -2 3                           $vertebrae cylinder
  13    2   -2.06 -20 2 -5                           $neck vertebrae
  14    2   -2.06 -37 38 23 -24 #12                  $rib
  15    2   -2.06 -21 22 25 -26 #12                  $rib
  16    2   -2.06 -21 22 27 -28 #12                  $rib
  17    2   -2.06 -21 22 29 -30 #12                  $rib
  18    2   -2.06 -21 22 31 -32 #12                  $rib
  19    2   -2.06 -21 22 33 -34 #12                  $rib
  20    2   -2.06 -21 22 35 -36 #12                  $rib
 115    2   -2.06 -46 47 -125 126 #12                $rib
 116    2   -2.06 -45 46 -127 128 #12                $rib
 117    2   -2.06 -44 45 -129 130 #12                $rib
 118    2   -2.06 -43 44 -131 132 #12                $rib
 119    2   -2.06 -41 42 -133 134 #12                $rib
 120    2   -2.06 -39 40 -135 136 #12                $rib
  21    2   -2.06 138 -139 -48 49 -50 51             $shoulder
  22    2   -2.06 -140 141 -48 49 -50 51             $shoulder
c  23    3   -3.67 142 -143 144 -145 146 -147  $detector
  24    2   -2.06 -12 7 -8 #115
  25    2   -2.06 -13 7 -8 #15
```

```
 26    2   -2.06 -14 7 -8 #15
 27    2   -2.06 -15 7 -8 #115                    $femur
 23    3   -3.67 151 -152 161 -162 -157 158    $detectors
 28    3   -3.67 151 -152 161 -162 -159 160
 29    3   -3.67 153 -154 161 -162 -157 158
 30    3   -3.67 153 -154 161 -162 -159 160
 31    3   -3.67 155 -156 161 -162 -157 158
 32    3   -3.67 155 -156 161 -162 -159 160
c  33    3   -3.67 +162 -163 -165 +166 +169 -170
c 34    3   -3.67 +164 -212 -167 +168 +169 -170
201    5 -0.001293 205 -206 209 -210 202 -201
202    6  -7.874 203 -204 207 -208 202 -201 #201
203    5 -0.001293 213 -214 209 -210 202 -201
204    6  -7.874 211 -212 207 -208 202 -201 #203
205    5 -0.001293 203 -212 209 -210 216 -217
206    6  -7.874 203 -212 207 -208 201 -215 #205
207    5 -0.001293 221 -222 209 -224 202 -218
208    6  -7.874 219 -220 207 -223 202 -218 #207
209    5 -0.001293 228 -219 209 -224 227 -226
210    6  -7.874 228 -219 207 -223 225 -218 #209
211    5 -0.001293 232 -233 209 -224 230 -229
212    6  -7.874 231 -228 207 -223 230 -229 #211
213    5 -0.001293 234 -231 209 -224 237 -236
214    6  -7.874 234 -231 207 -223 235 -229 #213
215    5 -0.001293 239 -240 209 -224 230 -229
216    6  -7.874 238 -234 207 -223 230 -229 #215
217    5 -0.001293 -242 243 -219
218    6  -7.874 -241 243 -219 #217
219    5 -0.001293 -245 202 -229
220    6  -7.874 -244 202 -229 #219
221    5 -0.001293 249 -250 209 -224 230 -246
222    6  -7.874 247 -248 207 -223 230 -246 #221
223    5 -0.001293 243 -247 209 -224 253 -252
224    6  -7.874 243 -247 207 -223 251 -246 #223
225    5 -0.001293 -255 256 -257
226    6  -7.874 -254 256 -257 #225
227    5 -0.001293 -259 243 -247
228    6  -7.874 -258 243 -247 #227
229    5 -0.001293 243 -247 209 -224 263 -262
230    6  -7.874 243 -247 207 -223 261 -260 #229
231    5 -0.001293 243 -247 209 -224 267 -266
232    6  -7.874 243 -247 207 -223 265 -264 #231
233    6  -7.874 243 -247 224 -223 264 -261
234    5 -0.001293 -269 271 -270
```

```
235     6  -7.874 -268 271 -270 #234
236     5 -0.001293 -273 271 -270
237     6  -7.874 -272 271 -270 #236
238     5 -0.001293 -275 271 -270
239     6  -7.874 -274 271 -270 #238
240     5 -0.001293 -277 230 -246
241     6  -7.874 -276 230 -246 #240
242     5 -0.001293 280 -281 209 -224 230 -246
243     6  -7.874 278 -279 207 -223 230 -246 #242
244     5 -0.001293 282 -278 209 -224 253 -252
245     6  -7.874 282 -278 207 -223 251 -246 #244
246     5 -0.001293 -259 282 -278
247     6  -7.874 -258 282 -278 #246
248     5 -0.001293 282 -278 209 -224 263 -262
249     6  -7.874 282 -278 207 -223 261 -260 #248
250     6  -7.874 282 -278 224 -223 264 -283
251     5 -0.001293 282 -278 209 -224 267 -266
252     6  -7.874 282 -278 207 -223 265 -264 #251
253     5 -0.001293 -285 271 -270
254     6  -7.874 -284 271 -270 #253
255     5 -0.001293 -287 271 -270
256     6  -7.874 -286 271 -270 #255
257     5 -0.001293 -289 271 -270
258     6  -7.874 -288 271 -270 #257
259     5 -0.001293 -291 271 -270
260     6  -7.874 -290 271 -270 #259
261     5 -0.001293 -293 271 -270
262     6  -7.874 -292 271 -270 #261
263     5 -0.001293 -295 271 -270
264     6  -7.874 -294 271 -270 #263
265     5 -0.001293 -297 271 -270
266     6  -7.874 -296 271 -270 #265
267     5 -0.001293 -299 271 -270
268     6  -7.874 -298 271 -270 #267
269     5 -0.001293 -255 300 -301
270     6  -7.874 -254 300 -301 #269
271     5 -0.001293 -255 302 -303
272     6  -7.874 -254 302 -303 #271
273     5 -0.001293 -255 304 -305
274     6  -7.874 -254 304 -305 #273
275     5 -0.001293 -255 306 -307
276     6  -7.874 -254 306 -307 #275
277     6  -7.874 228 -219 224 -223 230 -225
278     6  -7.874 -308 312 -235 #244 #245
```

```
279    6  -7.874 -309 312 -235 #244 #245
280    6  -7.874 -310 312 -235 #244 #245
281    6  -7.874 -311 312 -235 #244 #245
282    6  -7.874 -313 312 -235 #223 #224
401    5 -0.001293 205 -206 -409 410 202 -201
402    6  -7.874 203 -204 -407 408 202 -201 #401
403    5 -0.001293 213 -214 -409 410 202 -201
404    6  -7.874 211 -212 -407 408 202 -201 #403
405    5 -0.001293 203 -212 -409 410 216 -217
406    6  -7.874 203 -212 -407 408 201 -215 #405
407    5 -0.001293 221 -222 -409 424 202 -218
408    6  -7.874 219 -220 -407 423 202 -218 #407
409    5 -0.001293 228 -219 -409 424 227 -226
410    6  -7.874 228 -219 -407 423 225 -218 #409
411    5 -0.001293 232 -233 -409 424 230 -229
412    6  -7.874 231 -228 -407 423 230 -229 #411
413    5 -0.001293 234 -231 -409 424 237 -236
414    6  -7.874 234 -231 -407 423 235 -229 #413
415    5 -0.001293 239 -240 -409 424 230 -229
416    6  -7.874 238 -234 -407 423 230 -229 #415
417    5 -0.001293 -442 243 -219
418    6  -7.874 -441 243 -219 #417
419    5 -0.001293 -445 202 -229
420    6  -7.874 -444 202 -229 #419
421    5 -0.001293 249 -250 -409 424 230 -246
422    6  -7.874 247 -248 -407 423 230 -246 #421
423    5 -0.001293 243 -247 -409 424 253 -252
424    6  -7.874 243 -247 -407 423 251 -246 #423
425    5 -0.001293 -455 256 -257
426    6  -7.874 -454 256 -257 #425
427    5 -0.001293 -459 243 -247
428    6  -7.874 -458 243 -247 #427
429    5 -0.001293 243 -247 -409 424 263 -262
430    6  -7.874 243 -247 -407 423 261 -260 #429
431    5 -0.001293 243 -247 -409 424 267 -266
432    6  -7.874 243 -247 -407 423 265 -264 #431
433    6  -7.874 243 -247 -424 423 264 -261
434    5 -0.001293 -469 271 -270
435    6  -7.874 -468 271 -270 #434
436    5 -0.001293 -473 271 -270
437    6  -7.874 -472 271 -270 #436
438    5 -0.001293 -475 271 -270
439    6  -7.874 -474 271 -270 #438
440    5 -0.001293 -477 230 -246
```

```
441    6  -7.874 -476 230 -246 #440
442    5 -0.001293 280 -281 -409 424 230 -246
443    6  -7.874 278 -279 -407 423 230 -246 #442
444    5 -0.001293 282 -278 -409 424 253 -252
445    6  -7.874 282 -278 -407 423 251 -246 #444
446    5 -0.001293 -459 282 -278
447    6  -7.874 -458 282 -278 #446
448    5 -0.001293 282 -278 -409 424 263 -262
449    6  -7.874 282 -278 -407 423 261 -260 #448
450    6  -7.874 282 -278 -424 423 264 -283
451    5 -0.001293 282 -278 -409 424 267 -266
452    6  -7.874 282 -278 -407 423 265 -264 #451
453    5 -0.001293 -485 271 -270
454    6  -7.874 -484 271 -270 #453
455    5 -0.001293 -487 271 -270
456    6  -7.874 -486 271 -270 #455
457    5 -0.001293 -489 271 -270
458    6  -7.874 -488 271 -270 #457
459    5 -0.001293 -491 271 -270
460    6  -7.874 -490 271 -270 #459
461    5 -0.001293 -493 271 -270
462    6  -7.874 -492 271 -270 #461
463    5 -0.001293 -495 271 -270
464    6  -7.874 -494 271 -270 #463
465    5 -0.001293 -497 271 -270
466    6  -7.874 -496 271 -270 #465
467    5 -0.001293 -499 271 -270
468    6  -7.874 -498 271 -270 #467
469    5 -0.001293 -455 300 -301
470    6  -7.874 -454 300 -301 #469
471    5 -0.001293 -455 302 -303
472    6  -7.874 -454 302 -303 #471
473    5 -0.001293 -455 304 -305
474    6  -7.874 -454 304 -305 #473
475    5 -0.001293 -455 306 -307
476    6  -7.874 -454 306 -307 #475
477    6  -7.874 228 -219 -424 423 230 -225
478    6  -7.874 -508 312 -235 #444 #445
479    6  -7.874 -509 312 -235 #444 #445
480    6  -7.874 -510 312 -235 #444 #445
481    6  -7.874 -511 312 -235 #444 #445
482    6  -7.874 -513 312 -235 #423 #424
998    5 -0.001293 -148 -149 16 -700 (1 :2 :-3 )(-4 :-2 :5 )(17 :18 :-5 )
       (6 :-7 :8 )(9 :-7 :8 )(10 :-7 :8 )(11 :-7 :8 )(12 :7 :-16 )
```

```
        (13 :7 :-16 )(14 :7 :-16 )(15 :7 :-16 )
        (-203 :204 :-207 :208 :-202 :201 )(-211 :212 :-207 :208 :-202
         :201 )(-203 :212 :-207 :208 :-201 :215 )(-219 :220 :-207 :223 :-202
         :218 )(-228 :219 :-207 :223 :-225 :218 )(-231 :228 :-207 :223 :-230
         :229 )(-234 :231 :-207 :223 :-235 :229 )(-238 :234 :-207 :223 :-230
         :229 )(241 :-243 :219 )(244 :-202 :229 )(-247 :248 :-207 :223 :-230
         :246 )(-243 :247 :-207 :223 :-251 :246 )(254 :-256 :257 )
        (258 :-243 :247 )(-243 :247 :-207 :223 :-261 :260 )
        (-243 :247 :-207 :223 :-265 :264 )(-243 :247 :-224 :223 :-264 :261 )
        (268 :-271 :270 )(272 :-271 :270 )(274 :-271 :270 )(276 :-230 :246 )
        (-278 :279 :-207 :223 :-230 :246 )(-282 :278 :-207 :223 :-251 :246 )
        (258 :-282 :278 )(-282 :278 :-207 :223 :-261 :260 )
        (-282 :278 :-224 :223 :-264 :283 )(-282 :278 :-207 :223 :-265 :264 )
        (284 :-271 :270 )(286 :-271 :270 )(288 :-271 :270 )(290 :-271 :270 )
        (292 :-271 :270 )(294 :-271 :270 )(296 :-271 :270 )(298 :-271 :270 )
        (254 :-300 :301 )(254 :-302 :303 )(254 :-304 :305 )(254 :-306 :307 )
        (-228 :219 :-224 :223 :-230 :225 )(308 :-312 :235 )(309 :-312 :235 )
        (310 :-312 :235 )(311 :-312 :235 )(313 :-312 :235 )
 997    5 -0.001293 -148 -149 16 700
        (-203 :204 :407 :-408 :-202 :201 )(-211 :212 :407 :-408 :-202 :201 )
        (-203 :212 :407 :-408 :-201 :215 )(-219 :220 :407 :-423 :-202 :218 )
        (-228 :219 :407 :-423 :-225 :218 )(-231 :228 :407 :-423 :-230 :229 )
        (-234 :231 :407 :-423 :-235 :229 )(-238 :234 :407 :-423 :-230 :229 )
        (441 :-243 :219 )(444 :-202 :229 )(-247 :248 :407 :-423 :-230 :246 )
        (-243 :247 :407 :-423 :-251 :246 )(454 :-256 :257 )(458 :-243 :247 )
        (-243 :247 :407 :-423 :-261 :260 )(-243 :247 :407 :-423 :-265 :264 )
        (-243 :247 :424 :-423 :-264 :261 )(468 :-271 :270 )(472 :-271 :270 )
        (474 :-271 :270 )(476 :-230 :246 )(-278 :279 :407 :-423 :-230 :246 )
        (-282 :278 :407 :-423 :-251 :246 )(458 :-282 :278 )
        (-282 :278 :407 :-423 :-261 :260 )(-282 :278 :424 :-423 :-264 :283 )
        (-282 :278 :407 :-423 :-265 :264 )(484 :-271 :270 )(486 :-271 :270 )
        (488 :-271 :270 )(490 :-271 :270 )(492 :-271 :270 )(494 :-271 :270 )
        (496 :-271 :270 )(498 :-271 :270 )(454 :-300 :301 )(454 :-302 :303 )
        (454 :-304 :305 )(454 :-306 :307 )(-228 :219 :424 :-423 :-230 :225 )
        (508 :-312 :235 )(509 :-312 :235 )(510 :-312 :235 )(511 :-312 :235 )
        (513 :-312 :235 ) #23 #28 #29 #30 #31 #32
 999    0       (148 :149 :-16 ) #301 #302 #303

c  --surface cards --
   1    2  sq 1 6.61151 6.61151 0 0 0 -7200 0 0 0
   2    2  px 54
   3    2  px -54
   4    2  gq -0.00496 -0.00276 -0.00276 1.7e-006 -1.2e-006 0.007643 0.486445
             -9.2e-005 -0.41273 -10
```

```
  5     2  px 73
  6     2 k/z -44 -16 -135.5 0.005739 0
  7     2  pz -49
  8     2  pz -16
  9     2 k/z 44 -16 -135.5 0.005739 0
 10     2 k/z 44 16 -135.5 0.005739 0
 11     2 k/z -44 16 -135.5 0.005739 0
 12     2 c/z -44 -16 5
 13     2 c/z 44 -16 5
 14     2 c/z 44 16 5
 15     2 c/z -44 16 5
 16     2  pz -82
 17     2 k/x 193.33 0 26.31 0.02493 0
 18     2  px 92
 19     2 c/x 0 20.6 3.5
 20     1  cx 3.5
 21     2  cx 24.1
 22     2  cx 23.1
 23     2  px 1.5
 24     2  px 4.5
 25     2  px 36.25
 26     2  px 39.25
 27     2  px 30.25
 28     2  px 33.25
 29     2  px 25.25
 30     2  px 28.25
 31     2  px 19.25
 32     2  px 22.25
 33     2  px 13.25
 34     2  px 16.25
 35     2  px 7.25
 36     2  px 10.25
 37     2 c/x 0 2 22.1
 38     2 c/x 0 2 21.1
 39     2 c/x 0 4 20.1
 40     2 c/x 0 4 19.1
 41     2 c/x 0 6 18.1
 42     2 c/x 0 6 17.1
 43     2 c/x 0 8 16.1
 44     2 c/x 0 8 15.1
 45     2 c/x 0 9 14.1
 46     2 c/x 0 10 13.1
 47     2 c/x 0 11 12.1
125     2  px -26.5
```

```
  126     2  px -29.5
  127     2  px -21.5
  128     2  px -24.5
  129     2  px -16.5
  130     2  px -19.5
  131     2  px -11.5
  132     2  px -14.5
  133     2  px -6.5
  134     2  px -9.5
  135     2  px -1.5
  136     2  px -4.5
c 137     2 c/y 46 12 3.5
  138     2  py 20
  139     2  py 21
  140     2  py -20
  141     2  py -21
   48     2  pz 15.0
   49     2  pz 3.0
   50     4  px 45.0
   51     5  px 42.5
c  142     2  px -20.32
c  143     2  px 20.32
c  144     2  py 50
c  145     2  py 55.08
c  146     2  pz -5.08
c  147     2  pz 5.08
  148        cz 1000
  149        pz 1000
  150        pz -90
  151        px -170.16
  152        px -160
  153        px -39.33
  154        px -29.17
  155        px 91.5
  156        px 101.66
  157        pz 39
  158        pz -1.64
  159        pz -35.36
  160        pz -76
  161        py 50
  162        py 55.08
  201        pz 92.5
  202        pz -82
  203        px -185
```

```
204     px -174.5
205     px -184.6
206     px -174.9
207     py -43
208     py -35
209     py -42.6
210     py -35.4
211     px 105
212     px 115.5
213     px 105.4
214     px 115.1
215     pz 103
216     pz 92.9
217     pz 102.6
218     pz 12.5
219     px 99.1
220     px 104.1
221     px 99.5
222     px 103.7
223     py -38
224     py -38.4
225     pz 7.5
226     pz 12.1
227     pz 7.9
228     px 86.6
229     pz 84.8
230     pz -77
231     px 81.6
232     px 82
233     px 86.2
234     px -98.68
235     pz 79.8
236     pz 84.4
237     pz 80.2
238     px -103.68
239     px -103.28
240     px -99.08
241    c/x -40.5 -79.5 2.5
242    c/x -40.5 -79.5 2.1
243     px -168.58
244    c/z -171.08 -40.5 2.5
245    c/z -171.08 -40.5 2.1
246     pz 75
247     px -109.58
```

```
248      px -104.58
249      px -109.18
250      px -104.98
251      pz 70
252      pz 74.6
253      pz 70.4
254     c/x -40.5 66.3 1.3
255     c/x -40.5 66.3 0.875
256      px -157
257      px -123
258     c/x -40.5 -7.5 2.5
259     c/x -40.5 -7.5 2.1
260      pz -15
261      pz -20
262      pz -15.4
263      pz -19.6
264      pz -70
265      pz -75
266      pz -70.4
267      pz -74.6
268     c/z -153.93 -40.5 2.16
269     c/z -153.93 -40.5 1.76
270      pz 64.98
271      pz -5
272     c/z -139.08 -40.5 2.16
273     c/z -139.08 -40.5 1.76
274     c/z -125.93 -40.5 2.16
275     c/z -125.93 -40.5 1.76
276     c/z -94.04 -40.5 3.74
277     c/z -94.04 -40.5 3.34
278      px 75.7
279      px 80.7
280      px 76.1
281      px 80.3
282      px -90.3
283      pz -21
284     c/z -74.2 -40.5 2.16
285     c/z -74.2 -40.5 1.76
286     c/z -57.1 -40.5 2.16
287     c/z -57.1 -40.5 1.76
288     c/z -32.7 -40.5 2.16
289     c/z -32.7 -40.5 1.76
290     c/z -15.6 -40.5 2.16
291     c/z -15.6 -40.5 1.76
```

```
292     c/z 8.8 -40.5 2.16
293     c/z 8.8 -40.5 1.76
294     c/z 25.9 -40.5 2.16
295     c/z 25.9 -40.5 1.76
296     c/z 50.3 -40.5 2.16
297     c/z 50.3 -40.5 1.76
298     c/z 67.4 -40.5 2.16
299     c/z 67.4 -40.5 1.76
300      px -78.95
301      px -52.35
302      px -37.45
303      px -10.85
304      px 4.05
305      px 30.65
306      px 45.5
307      px 72.15
308     c/z -65.65 -44.15 2.35
309     c/z -24.15 -44.15 2.35
310     c/z 17.35 -44.15 2.35
311     c/z 58.825 -44.15 2.35
312      pz 66
313     c/z -139.08 -44.15 2.35
407      py 43
408      py 35
409      py 42.6
410      py 35.4
423      py 38
424      py 38.4
441     c/x 40.5 -79.5 2.5
442     c/x 40.5 -79.5 2.1
444     c/z -171.08 40.5 2.5
445     c/z -171.08 40.5 2.1
454     c/x 40.5 66.3 1.3
455     c/x 40.5 66.3 0.875
458     c/x 40.5 -7.5 2.5
459     c/x 40.5 -7.5 2.1
468     c/z -153.93 40.5 2.16
469     c/z -153.93 40.5 1.76
472     c/z -139.08 40.5 2.16
473     c/z -139.08 40.5 1.76
474     c/z -125.93 40.5 2.16
475     c/z -125.93 40.5 1.76
476     c/z -94.04 40.5 3.74
477     c/z -94.04 40.5 3.34
```

```
 484      c/z -74.2 40.5 2.16
 485      c/z -74.2 40.5 1.76
 486      c/z -57.1 40.5 2.16
 487      c/z -57.1 40.5 1.76
 488      c/z -32.7 40.5 2.16
 489      c/z -32.7 40.5 1.76
 490      c/z -15.6 40.5 2.16
 491      c/z -15.6 40.5 1.76
 492      c/z 8.8 40.5 2.16
 493      c/z 8.8 40.5 1.76
 494      c/z 25.9 40.5 2.16
 495      c/z 25.9 40.5 1.76
 496      c/z 50.3 40.5 2.16
 497      c/z 50.3 40.5 1.76
 498      c/z 67.4 40.5 2.16
 499      c/z 67.4 40.5 1.76
 508      c/z -65.65 44.15 2.35
 509      c/z -24.15 44.15 2.35
 510      c/z 17.35 44.15 2.35
 511      c/z 58.825 44.15 2.35
 513      c/z -139.08 44.15 2.35
 700      py  35
 701 RPP -284.7500  215.2500 -250.000  250.000 -112.48 -102.32  $ concrete slab
"layer 1"
 702 RPP -284.7500  215.2500 -250.000  250.000 -102.32  -92.16  $ concrete slab
"layer 2"
 703 RPP -284.7500  215.2500 -250.000  250.000 -92.16   -82     $ concrete slab "layer
3"

c  -- data cards --
mode  p
m1    1000.           0.632  $MAT1
     8000.          0.25893 6000.          0.09543 7000.          0.01364
m2    20000.         0.06224  $MAT2
     15000.          0.2886 8000.           0.646 1000.          0.00316
m3    11000.           0.5  $MAT3
     53000.           0.5
m6    26054.           0.058  $MAT6
     26056.          0.9172 26057.           0.022 26058.           0.28
m5    7000.            0.78  $MAT5
     8000.            0.21 1000.            0.01
c   -- Concrete --
c   --- F1 ---
m7    01000 -0.005000  $ Hydrogen in Concrete
```

```
      06000 -0.162900  $ Carbon in Concrete
      08000 -0.484500  $ Oxygen in Concrete
      11000 -0.000260  $ Sodium in Concrete
      12000 -0.011900  $ Magnesium in Concrete
      13000 -0.004440  $ Aluminum in Concrete
      14000 -0.015100  $ Silicon in Concrete
      19000 -0.001087  $ Potassium in Concrete
      20000 -0.310100  $ Calcium in Concrete
      25000 -0.000304  $ Manganese in Concrete
      26000 -0.004366  $ Iron in Concrete
c   --- F2 ---
c m1    01000 -0.005000  $ Hydrogen in Concrete
c       06000 -0.146100  $ Carbon in Concrete
c       08000 -0.487200  $ Oxygen in Concrete
c       11000 -0.000324  $ Sodium in Concrete
c       12000 -0.010600  $ Magnesium in Concrete
c       13000 -0.006236  $ Aluminum in Concrete
c       14000 -0.018600  $ Silicon in Concrete
c       19000 -0.001683  $ Potassium in Concrete
c       20000 -0.318800  $ Calcium in Concrete
c       25000 -0.000355  $ Manganese in Concrete
c       26000 -0.005406  $ Iron in Concrete
c   --- G1 ---
c m1    01000 -0.005000  $ Hydrogen in Concrete
c       06000 -0.023300  $ Carbon in Concrete
c       08000 -0.472700  $ Oxygen in Concrete
c       11000 -0.018700  $ Sodium in Concrete
c       12000 -0.003781  $ Magnesium in Concrete
c       13000 -0.061800  $ Aluminum in Concrete
c       14000 -0.266200  $ Silicon in Concrete
c       19000 -0.026600  $ Potassium in Concrete
c       20000 -0.100600  $ Calcium in Concrete
c       25000 -0.000785  $ Manganese in Concrete
c       26000 -0.021300  $ Iron in Concrete
c   --- G2 ---
c m1    06000 -0.000500  $ Carbon in Concrete
c       08000 -0.473100  $ Oxygen in Concrete
c       11000 -0.020000  $ Sodium in Concrete
c       12000 -0.003594  $ Magnesium in Concrete
c       13000 -0.066000  $ Aluminum in Concrete
c       14000 -0.295200  $ Silicon in Concrete
c       19000 -0.032700  $ Potassium in Concrete
c       20000 -0.089800  $ Calcium in Concrete
c       25000 -0.001153  $ Manganese in Concrete
```

```
c       26000 -0.019100  $ Iron in Concrete
c   --- L1 ---
c m1    01000 -0.005000  $ Hydrogen in Concrete
c       06000 -0.142900  $ Carbon in Concrete
c       08000 -0.476900  $ Oxygen in Concrete
c       11000 -0.000732  $ Sodium in Concrete
c       12000 -0.010900  $ Magnesium in Concrete
c       13000 -0.015300  $ Aluminum in Concrete
c       14000 -0.047500  $ Silicon in Concrete
c       19000 -0.006900  $ Potassium in Concrete
c       20000 -0.284800  $ Calcium in Concrete
c       25000 -0.000482  $ Manganese in Concrete
c       26000 -0.009090  $ Iron in Concrete
c   --- L2 ---
c m1    01000 -0.005000  $ Hydrogen in Concrete
c       06000 -0.119400  $ Carbon in Concrete
c       08000 -0.482100  $ Oxygen in Concrete
c       11000 -0.001022  $ Sodium in Concrete
c       12000 -0.008900  $ Magnesium in Concrete
c       13000 -0.017400  $ Aluminum in Concrete
c       14000 -0.053300  $ Silicon in Concrete
c       19000 -0.007705  $ Potassium in Concrete
c       20000 -0.294600  $ Calcium in Concrete
c       25000 -0.000501  $ Manganese in Concrete
c       26000 -0.001507  $ Iron in Concrete
*tr1 -66.9 0 13.155 60 90 30 90 0 90 150 90 60
*tr2 -130 0 0 0 90 90 90 0 90 90 90 0
*tr4 -130 0 0 15 90 105 90 0 90 75 90 15
*tr5 -130 0 0 15 90 75 90 0 90 105 90 15
imp:p   1 2 4 204r      0            $ 1, 999
sdef par 2 X d1 Y d2 Z d3 ERG d4
si1 -284.75 215.25
sp1  0 1
si2 -250 250
sp2  0 1
si3 -112.48 -82
sp3  0 1
Si4     L 0.09259 0.18621 0.23863 0.24200 0.29522 0.30009
        0.33832 0.35193 0.58319 0.60931 0.72733 0.91120
        0.96897 1.12029 1.23811 1.40799 1.46082 1.76449
        2.20406 2.61451
Sp4     D 0.00050 0.00069 0.00312 0.02023 0.05355 0.00024
        0.00111 0.10238 0.20460 0.18382 0.00978 0.00255
        0.00156 0.06021 0.02309 0.00857 0.00323 0.06141
```

```
        0.02026 0.24011
c sdef pos=91.999 0 28 erg=0.662
c sdef pos=0 0 -33 erg=0.662
c sdef pos=-50 -26.8042 1.2348 erg=0.662
c sdef pos=-40 -29.2784 1.6461 erg=0.662
c sdef pos=0 -33 0 erg=0.662
f8:p 23 28 29 30 31 32
e8 0 1.0e-06 0.01 32I 0.662 0.682 0.702 0.722 0.742 0.762
ft8 GEB 0 0.0691 -0.0951
nps 2E8
PRDMP 1e8 1e8
```

APPENDIX B

Sources present in the concrete and their corresponding specific activities are listed.

Nuclide	**Specific Activity (µCi/Kg of concrete)**	**Nuclide**	**Specific Activity (µCi/Kg of concrete)**
K-40	2.137	Bi-214	2.331
Tl-208	0.715	Bi-214	0.764
Tl-208	0.839	Bi-214	0.293
Pb-212	1.020	Bi-214	0.109
Pb-212	0.077	Bi-214	0.779
Pb-212	0.265	Bi-214	0.257
Bi-212	0.242	Ra-226	0.182
Pb-214	0.376	Ac-228	0.608
Pb-214	0.976	Ac-228	0.372
Pb-214	1.901	Th-234	0.336

VITA

Name:	Joe Justina
Address:	Texas A&M University Department of Nuclear Engineering 129 Zachry Engineering Center 3133 TAMU College Station, TX 77843-3133
Email Address:	joejustina@gmail.com
Education:	B.S., University of Mysore, India, 2007 M.Sc., Radiation Physics, Mangalore University, India, 2009 M.S., Nuclear Engineering, Texas A&M University, 2012